TECHNICAL REPORT H-68-2

HYDRAULIC CHARACTERISTICS OF MOBILE BREAKWATERS COMPOSED OF TIRES OR SPHERES

Hydraulic Laboratory Investigation

by

A. M. Kamel
D. D. Davidson

June 1968

Sponsored by

Office, Chief of Engineers
U. S. Army

Conducted by

U. S. Army Engineer Waterways Experiment Station
CORPS OF ENGINEERS
Vicksburg, Mississippi

ARMY-MRC VICKSBURG, MISS.

FOREWORD

Authority for the U. S. Army Engineer Waterways Experiment Station to perform this investigation was granted by the Office, Chief of Engineers (OCE), in a second indorsement dated 30 September 1966 to OCE letter dated 31 August 1966, subject, "Wave Maze Instrumentation." The investigation was conducted in the Water Waves Branch, Hydraulics Division, of the Waterways Experiment Station under the direction of Mr. E. P. Fortson, Jr., Chief of the Hydraulics Division, and Mr. R. Y. Hudson, Chief of the Water Waves Branch. The tests were performed during the period January-May 1967 by Mr. D. D. Davidson, project engineer, under the supervision of Dr. A. M. Kamel, Special Assistant to the Chief of the Hydraulics Division. This report was prepared by Dr. Kamel and Mr. Davidson.

Liaison with the Office, Chief of Engineers, was maintained throughout the course of the investigation by means of progress reports and conferences. Mr. C. E. Lee, Assistant Chief, Hydraulic Design Branch, Engineering Division, Civil Works, Office, Chief of Engineers, visited the Waterways Experiment Station at various times in connection with the investigation.

Director of the Waterways Experiment Station during the conduct of this investigation and the preparation of this report was COL John R. Oswalt, Jr., CE. Technical Director was Mr. J. B. Tiffany.

CONTENTS

	Page
FOREWORD	v
NOTATION	ix
CONVERSION FACTORS, BRITISH TO METRIC UNITS OF MEASUREMENT	xiii
SUMMARY	xv
PART I: INTRODUCTION	1
Background	1
Purpose and Scope of Study	3
PART II: ANALYTICAL CONSIDERATIONS	4
Wave Amplitude	4
Power Dissipated	7
Mooring Line Forces	7
Variables Affecting Efficiency of Mobile Breakwaters Tested	9
PART III: EXPERIMENTAL EQUIPMENT AND PROCEDURES	10
Wave Channel and Wave Generator	10
Measuring Apparatus	10
Experimental Procedures	11
Selected Test Conditions	11
Breakwater Sections Tested	12
PART IV: ANALYSIS OF TEST RESULTS	19
Effect of h/d, y/d, and H_i/L on Reflection and Transmission Coefficients, Tire Assembly	21
Variation of Reflection Coefficient with H_i/L for Different Values of w/L and y/d, Tire and Sphere Assemblies	23
Variation of Transmission Coefficient with H_i/L for Different Values of w/L and y/d, Tire and Sphere Assemblies	24
Variation of Power Dissipated by Breakwater with H_i/L for Different Values of w/L and y/d, Tire and Sphere Assemblies	25
Variation of Force in Mooring Lines with w/L, Tire and Sphere Assemblies	27
PART V: CONCLUSIONS	29

CONTENTS

LITERATURE CITED . . . . . .

TABLES 1-4

PLATES 1-23

NOTATION

a_n Wave amplitude; n = 1, 2, 3, 4

a_1 Amplitude of incident wave

a_2 Amplitude of wave reflected by breakwater

a_3 Amplitude of wave transmitted through breakwater

a_4 Amplitude of wave reflected by absorber beach

b_1 Width of breakwater

C_G Wave group velocity

d Water depth

e Porosity of breakwater (percent voids)

f_{cn} Maximum force in mooring line of breakwater per unit area of breakwater section perpendicular to direction of wave propagation;

$n = 1, 2 ; f_{cn} = \frac{F_n}{b(y + h)}$

f_{c1} Maximum force in seaward mooring line of breakwater per unit of breakwater section perpendicular to direction of wave propagation;

$$f_{c1} = \frac{F_1}{b(y + h)}$$

f_{c2} Maximum force in shoreward mooring line of breakwater per unit area of breakwater section perpendicular to direction of wave propagation;

$$f_{c2} = \frac{F_2}{b(y + h)}$$

$f_{t_{max}}$ Theoretical maximum total horizontal force exerted on a total reflecting vertical wall per unit area of flow cross section perpendicular to direction of wave propagation; $f_{t_{max}} = F_{t_{max}} / bd$

F_n Maximum force in mooring line of breakwater; n = 1, 2

F_1	Maximum force in seaward mooring line of breakwater
F_2	Maximum force in shoreward mooring line of breakwater
$F_{t_{max}}$	Theoretical maximum total horizontal force exerted on a totally reflecting vertical wall
g	Gravitational constant = 32.2 ft/sec^2
h	Distance to which breakwater extends above water surface
H_i	Height of incident wave
H_r	Height of reflected wave
H_t	Height of transmitted wave
k	Wave parameter defined as $2\pi/L$
K_r	Wave reflection coefficient
K_t	Wave transmission coefficient
L	Wavelength
p	Pressure beneath a wave
P	Power of incident wave
P_D	Wave power dissipated by breakwater
P_z	Wave power above a depth
swl	Still-water level
t	Time
T	Wave period
w	Length of breakwater in direction of wave propagation
x	Horizontal coordinate, positive in direction of propagation of incident wave
y	Distance to which breakwater extends below water surface
z	Vertical coordinate, positive upward
γ	Specific weight of water

ϵ_n Phase angle

η_x Displacement of envelope of wave amplitude from still-water level

π Numerical constant, 3.14159 or 3.1416

σ Angular frequency = $2\pi/T$

ψ, ϕ Functions

CONVERSION FACTORS, BRITISH TO METRIC UNITS OF MEASUREMENT

British units of measurement used in this report can be converted to metric units as follows:

Multiply	By	To Obtain
inches	2.54	centimeters
feet	0.3048	meters
pounds	0.45359237	kilograms
Fahrenheit degrees	5/9	Celsius or Kelvin degrees*

* To obtain Celsius (C) temperature readings from Fahrenheit (F) readings, use the following formula: $C = (5/9)(F - 32)$. To obtain Kelvin (K) readings, use $K = (5/9)(F - 32) + 273.16$.

SUMMARY

Two new types of mobile breakwaters consisting of tire and sphere assemblies, respectively, were tested. Tests covered a wide range of wave conditions, water depths, and breakwater dimensions. Experimental measurements were made to determine the wave reflection and wave transmission coefficients, the power dissipated by the breakwaters, and the forces in the mooring lines of the breakwaters. It was found that for these types of floating breakwaters to be effective their length should be on the order of one-half to one wavelength, their depth on the order of half the water depth, and the wave steepness equal to or greater than about 0.04. The effectiveness of these breakwaters can be improved by decreasing their porosity and flexibility; however, this would cause an increase in the mooring forces and the drift, the drift being the result of the difference between the forces in the seaward and shoreward mooring lines.

HYDRAULIC CHARACTERISTICS OF MOBILE BREAKWATERS COMPOSED OF TIRES OR SPHERES

Hydraulic Laboratory Investigation

PART I: INTRODUCTION

Background

1. Harbors and shorelines can be protected by reducing the height of the waves to which they are exposed. This can be achieved by use of breakwaters, fixed or mobile. Fixed breakwaters occupy the full depth and can be built as solid, nearly vertical walls reflecting the wave energy, or as rubble mounds with sloping faces inducing partial breaking. Often a combination of these is employed. The cost of building fixed breakwaters is high and is justified only for permanent installations. The lower parts of these full-depth breakwaters are sometimes ineffective with respect to wave action (since the wave energy is concentrated near the surface for short-period waves in relatively deep water) and, in some cases, serve to cut off underwater currents and cause undesirable erosion and deposition of bottom sediments.[1]

2. The need by both military and civil works projects for a breakwater which will offer adequate wave protection, but which will exhibit the desirable features of mobility, ease of assembly, and moderate cost, has amplified the search for mobile breakwaters in recent years. A mobile breakwater is defined as a structure or device that combines the ability to appreciably reduce the height of waves in its lee with a degree of mobility sufficient to permit its ready transportation for considerable distances and its speedy installation.[2] Several attempts have been made to achieve the requirements of a mobile breakwater,[3-10] some with a fair degree of success. A considerable effort in this direction was made during World War II, which resulted in the development of the "Phoenix" and "Bombardon" breakwaters used in the Normandy invasion.

3. Mobile breakwaters can cause attenuation of wave height by one

of more of the following methods: wave reflection, dissipation of wave energy by breaking, destruction of wave orbital motion, out-of-phase damping, and viscous damping. Examples of each of these methods are shown in plate 1.

4. Recently, two mobile breakwaters were developed based on the method of wave attenuation by destruction of orbital motion. The first consists of an assembly of used tires (fig. 1) known as the Wave Maze.

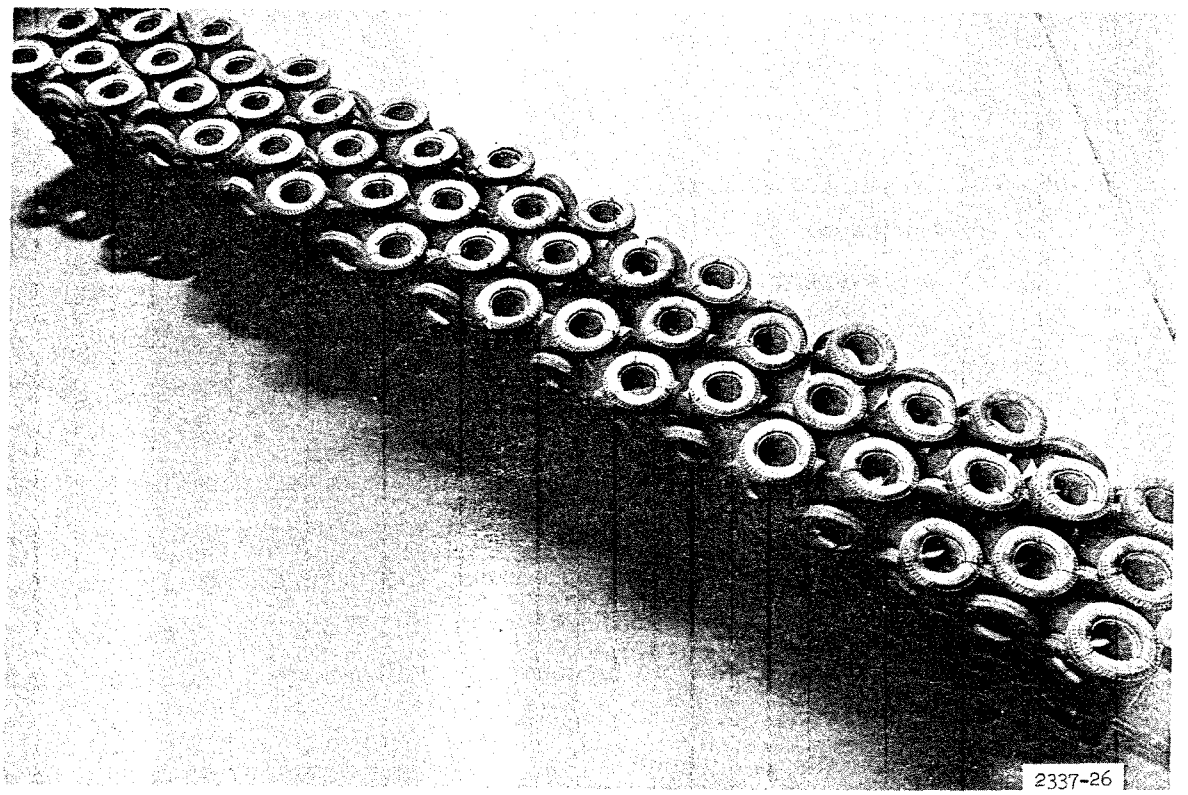

Fig. 1. Model of mobile breakwater consisting of an assembly of tires

It was developed and patented on the West Coast,[12] and a prototype assembly constructed in Tomales Bay, California, was claimed to be an effective wave attenuator for wave conditions in that area. The second consists of an assembly of spheres (fig. 2) and was developed at the Waterways Experiment Station mainly for the purpose of comparing its performance with that of the Wave Maze.

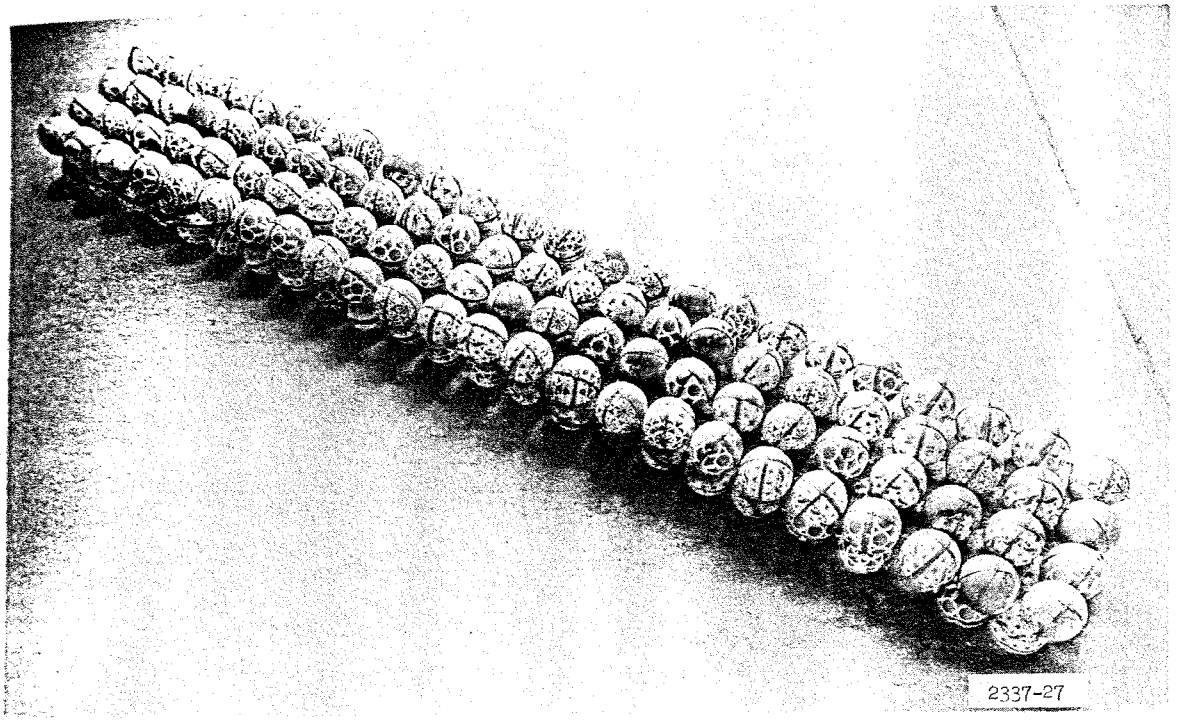

Fig. 2. Model of mobile breakwater consisting of an assembly of spheres

Purpose and Scope of Study

5. The purpose of this pilot investigation was to obtain an appraisal of the effectiveness of mobile breakwaters consisting of tire or sphere assemblies. Specifically, it was desired to establish the range of conditions (wave steepness, wave period, water depth, and length, depth, and porosity of breakwater structure) under which these types of breakwaters can provide adequate wave protection.

PART II: ANALYTICAL CONSIDERATIONS

6. The mathematical derivations appearing in the following pages are taken from reference 1. They are presented here for easy reference by the interested reader.

Wave Amplitude

7. The amplitudes of the incident and reflected waves in a wave system (fig. 3) can be determined by using a single wave rod, recording

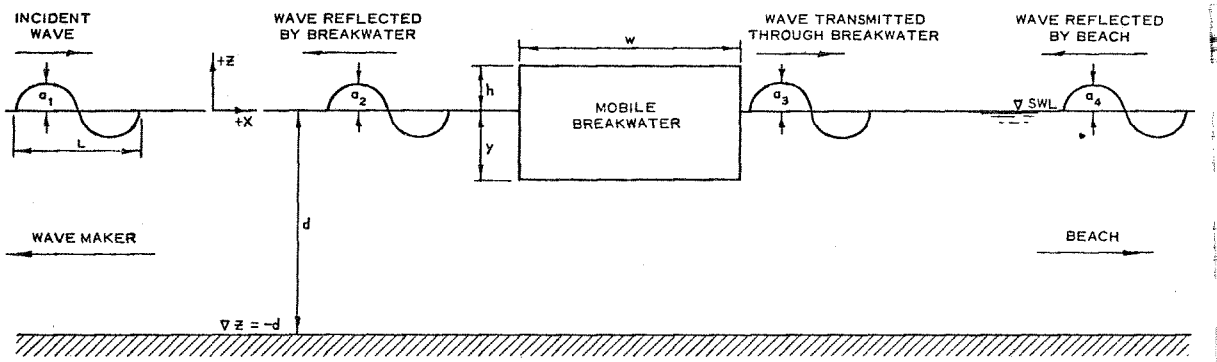

Fig. 3. Definition sketch for wave system

the fluctuations of the water surface while moving along the channel axis for a distance not less than one-fourth of a wavelength (fig. 4). The amplitudes can then be obtained from the recorded wave envelopes (fig. 5) as follows. Assuming that the incident and the reflected waves are of a sinusoidal form, they both must have the same period and can be expressed as

$$\eta_1 = a_1 \sin (kx - \sigma t - \sigma\epsilon_1) \qquad (1)$$

$$\eta_2 = a_2 \sin (kx + \sigma t + \sigma\epsilon_2) \qquad (2)$$

The phase angle for reflection is assumed to be equal to π ; therefore,

$$\eta = \eta_1 + \eta_2 = a_1(\sin kx \cos \sigma t - \cos kx \sin \sigma t) + a_2(\sin kx \cos \sigma t + \cos kx \sin \sigma t) \qquad (3)$$

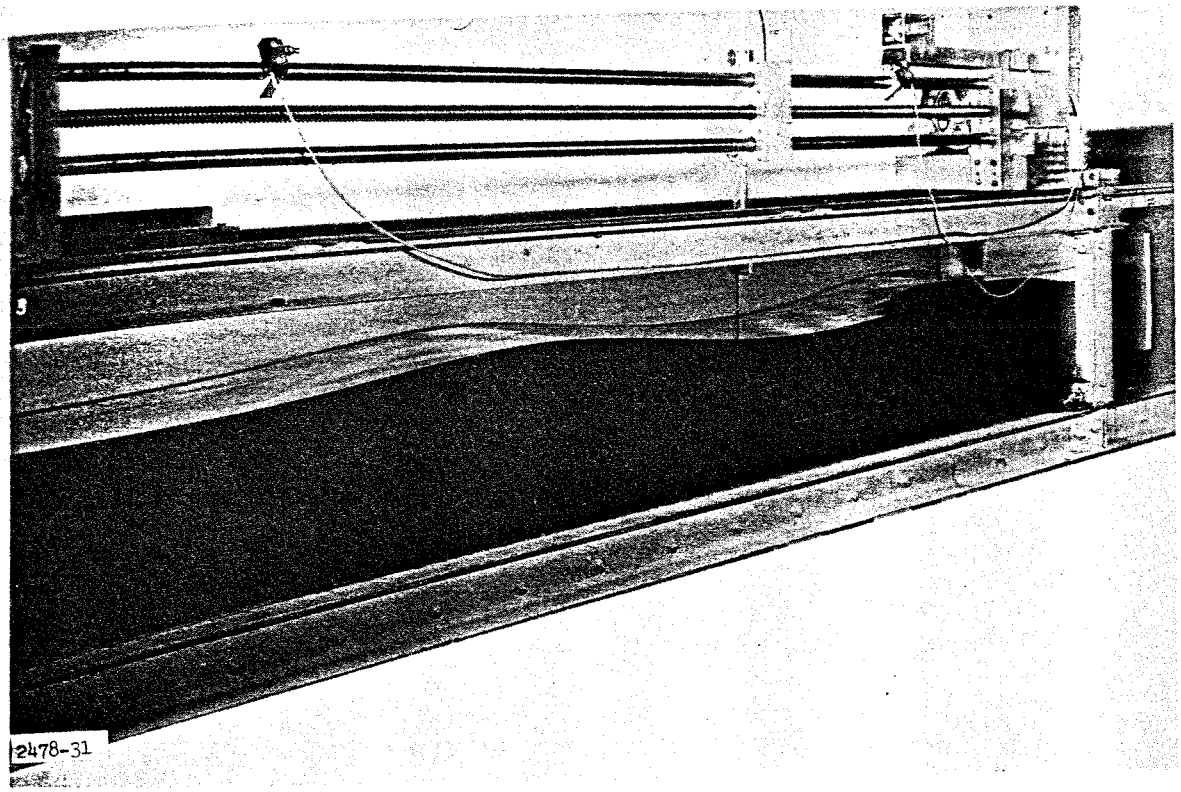

Fig. 4. Movable wave rod for recording fluctuations of water surface

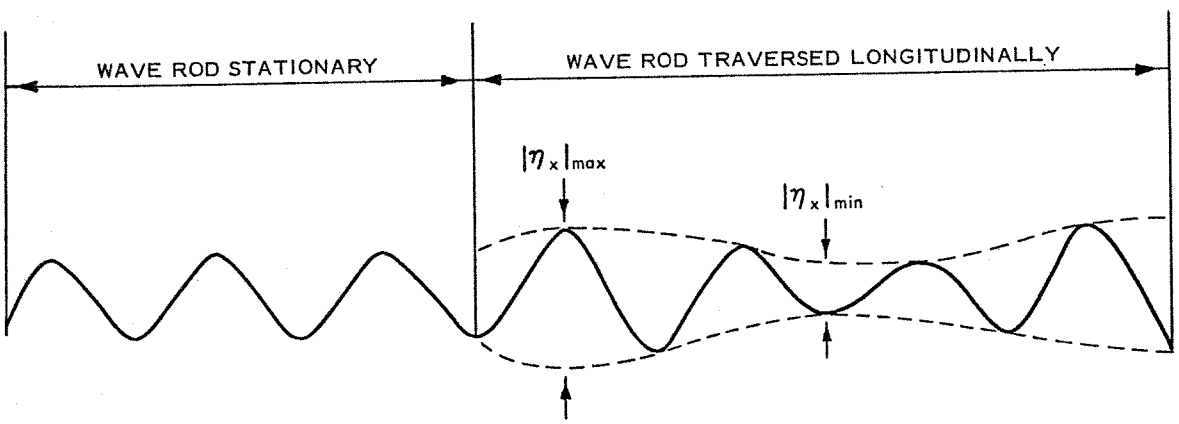

INCIDENT WAVE HEIGHT $H_i = 2a_1 = |\eta_x|_{max} + |\eta_x|_{min}$

REFLECTED WAVE HEIGHT $H_r = 2a_2 = |\eta_x|_{max} - |\eta_x|_{min}$

Fig. 5. Comparison of wave measurements recorded by stationary wave rod and by movable wave rod

Differentiating equation 3 with respect to the time t and setting the result equal to zero, the time at which this combined wave system produces maxima and minima is

$$\tan \sigma t_{max} = \frac{(a_2 - a_1) \cot kx}{(a_1 + a_2)} \tag{4}$$

Substituting the values of $\sin \sigma t_{max}$ and $\cos \sigma t_{max}$ obtained from equation 4 in equation 3, the equation for the variation of wave amplitude with distance is

$$\left|\eta_x\right| = \sqrt{(a_1 + a_2)^2 \sin^2 kx + (a_1 - a_2)^2 \cos^2 kx} \tag{5}$$

Differentiating equation 5 with respect to x and setting the result equal to zero, the maximum and minimum values of η_x are

$$\left|\eta_x\right|_{min} = a_1 - a_2 \quad \text{(occurs when } kx = n\pi \text{ ; } n = 0, 1, 2, \ldots) \tag{6}$$

$$\left|\eta_x\right|_{max} = a_1 + a_2 \quad \text{(occurs when } kx = \frac{2n + 1}{2}\pi \text{ ; } n = 0, 1, 2, \ldots) \tag{7}$$

From equations 6 and 7

$$a_1 = \frac{1}{2}\left(\left|\eta_x\right|_{max} + \left|\eta_x\right|_{min}\right) \tag{8}$$

and

$$a_2 = \frac{1}{2}\left(\left|\eta_x\right|_{max} - \left|\eta_x\right|_{min}\right) \tag{9}$$

8. Recording the wave envelopes upstream and downstream of the test structure, the reflection and transmission coefficients, respectively, can be obtained as

$$K_r = \frac{a_2}{a_1} \tag{10}$$

$$K_t = \frac{a_3}{a_1} \tag{11}$$

In the present study it was found that a_4, the amplitude of the wave reflected by the absorber beach, was of negligible magnitude. Therefore, the amplitude of the transmitted wave, a_3, was recorded using a fixed wave rod located downstream of the breakwater.

Power Dissipated

9. The power dissipated by the breakwater can be computed from the following expression: power incident = power transmitted + power reflected + power dissipated. That is,

$$\frac{\gamma a_1^2}{2} C_G = \frac{\gamma a_3^2}{2} C_G + \frac{\gamma a_2^2}{2} C_G + P_D \tag{12}$$

Equation 12 can be written

$$\frac{P_D}{P} = \frac{P_D}{\frac{\gamma a_1^2}{2} C_G} = 1 - \left(\frac{a_3}{a_1}\right)^2 - \left(\frac{a_2}{a_1}\right)^2 \tag{13}$$

Since $K_t = \frac{a_3}{a_1}$ and $K_r = \frac{a_2}{a_1}$, equation 13 becomes

$$\frac{P_D}{P} = 1 - K_t^2 - K_r^2 \tag{14}$$

The ratio of power above any depth, z, to the total power in the cross section is given by

$$\frac{P_z}{P} = \frac{1 - \left[\frac{\sinh 2k(d + z) + 2kz}{\sinh 2kd}\right]}{1 + \left(\frac{2kd}{\sinh 2kd}\right)} \tag{15}$$

Mooring Line Forces

10. A convenient way of studying the mooring line forces on the

structure tested is to determine the ratio of the maximum horizontal forces exerted on the structure to the maximum force that would exist in the case of a total reflection from a vertical wall. The maximum horizontal force exerted on the structure can be determined by attaching a horizontal force gage to the test section. However, due to the difficulty in obtaining the desired force gage in time for completion of testing and since the determination of the mooring line forces was beyond the scope of this investigation, a force meter was attached to the mooring lines as shown in fig. 6 simply to obtain an understanding of the approximate order of

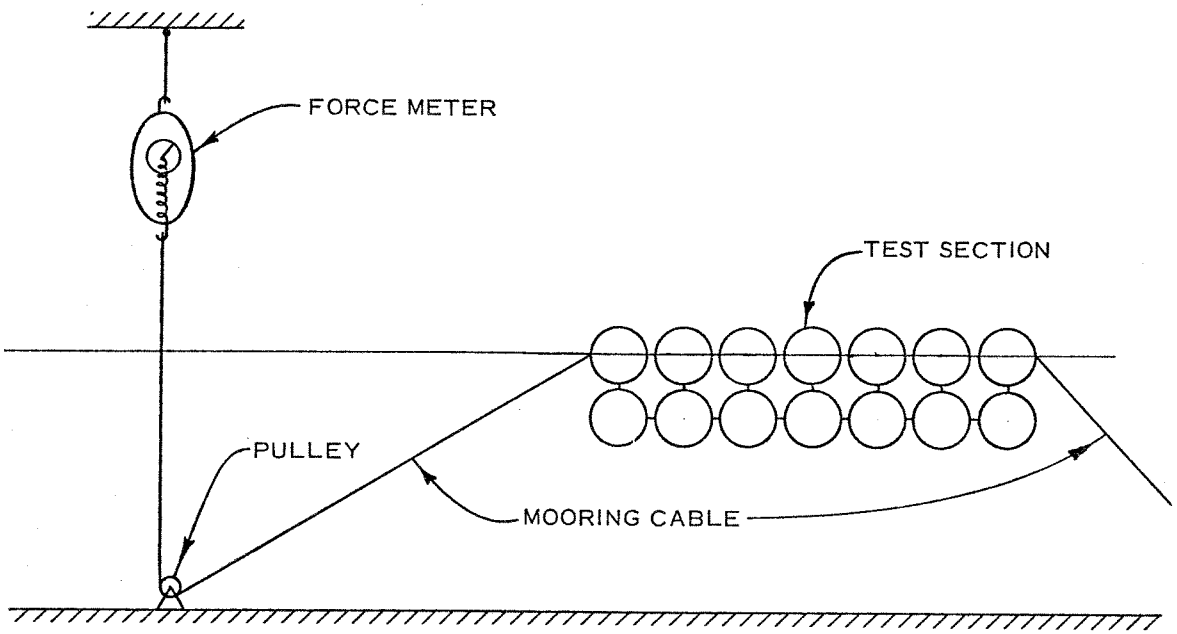

Fig. 6. Setup for mooring line force measurements

magnitude of these forces. The recorded mooring line forces were corrected to account for the fact that as the wave period approaches the natural period of the breakwater system, the indicated force is greater than the force actually experienced by the breakwaters. The value for the force on a vertical wall for total wave reflection of the incident wave per unit width of the channel is

$$f_t = \int_{-d}^{0} p \, dz \qquad (16)$$

The pressure beneath the wave, p , is

$$p = \gamma \left[\eta \frac{\cosh k(d + z)}{\cosh kd} - z \right] \tag{17}$$

Substituting equation 17 into equation 16 yields

$$f_t = \frac{\gamma \eta}{\cosh kd} \int_{-d}^{0} \cosh k(d + z) dz - \gamma \int_{-d}^{0} z \, dz \tag{18}$$

$$= \frac{\gamma \eta}{k \cosh kd} \sinh kd + \frac{\gamma d^2}{2} \tag{19}$$

The term $\frac{\gamma d^2}{2}$ is the hydrostatic pressure on the wall and is cancelled by the pressure exerted by the still water on the downstream face of the wall. The varying part of the total force on the wall, $\frac{\gamma \eta}{k} \tanh kd$, has a maximum value when

$$\eta = \eta_{max} = 2a_1 \tag{20}$$

Thus,

$$f_{t_{max}} = \frac{2a_1 \gamma}{k} \tanh kd = \frac{H_i \gamma}{k} \tanh kd \tag{21}$$

Variables Affecting Efficiency of Mobile Breakwaters Tested

11. The efficiency of the mobile breakwaters tested can be defined by the power dissipated by them, expressed as

$$P_D = \Psi(K_t, K_r) \tag{22}$$

That is,

$$P_D = \phi\left(\frac{d}{L}, \frac{H_i}{L}, \frac{w}{L}, \frac{y}{d}, \frac{h}{d}, e \right) \tag{23}$$

The different symbols are defined in the Notation (page ix) and shown in fig. 3.

PART III: EXPERIMENTAL EQUIPMENT AND PROCEDURES

Wave Channel and Wave Generator

12. Tests were conducted in a concrete wave channel, 150 ft* long, 2 ft wide, and 4.5 ft deep, with glass panels on one side. These glass viewing windows allowed photographing selected test conditions and visual observation of the action and reaction of the waves and test structures. The wave channel was equipped at one end with a power-driven, variable-speed and adjustable-stroke wave generator of the flap type. The wave absorber behind the wave generator consisted of a permeable, sloping rock mound. The wave absorber at the opposite end of the channel consisted of a permeable, sloping rock mound with a 4-in.-thick overlay of rubberized hair (plate 2).

Measuring Apparatus

13. Wave measurements were made using wave rods, amplifiers, and a multiple-channel oscillograph. Two types of wave rods were used--one fixed and one movable. The fixed rod, a parallel-wire type, was used for measuring the waves transmitted through the breakwater since reflection from the beach was of a negligible magnitude. The movable wave rod (fig. 4), known as the Saginaw screw, was used for measuring the height of the incident and reflected waves in front of the breakwater. The wave rod traversed along the axis of the channel for a distance not less than one-fourth a wavelength. The resulting wave trace showed the superpositioning of the incident and reflected waves. Fig. 5 shows an example of the two different traces recorded by the movable and fixed wave rods. The envelope of the crest and trough of the wave trace recorded by the movable wave rod has a minimum height $|\eta_x|_{min}$ and a maximum height $|\eta_x|_{max}$ from which the heights of the incident and reflected waves can be determined according to equations 8 and 9.

---

* A table of factors for converting British units of measurement to metric units is presented on page xiii.

Experimental Procedures

14. Each breakwater section tested was constructed to a width just under the 2-ft width of the channel to ensure its freedom of movement and was installed approximately two-thirds of the length of the channel from the wave generator. The breakwater sections were subjected to a variety of wave conditions as described in paragraph 15. For each test, the heights of the incident, reflected, and transmitted waves were measured to determine the reflection and transmission coefficients of the structure, $K_r = H_r/H_i$ and $K_t = H_t/H_i$, respectively. The mooring system consisted of stainless steel cables 1/16 in. in diameter threaded through a resistant pulley in the bottom of the flume and extended to a rigid support as shown in fig. 6. The slope of the mooring lines was arbitrarily selected to be 1:3 (one vertical and three horizontal).

Selected Test Conditions

15. Wave conditions used in the tests were varied over the maximum practical range permitted by the wave generator. The wave period, T, varied from 0.75 to 2.5 sec, which allowed a corresponding wavelength, L, to range from approximately 3 to 19 ft. The wave heights varied from 0.10 to 1.0 ft, and in terms of wave steepness, H_i/L, the test values varied from about 0.01 to 0.09. However, due to the wave generator limitations not all the steepnesses could be obtained for all the wave periods.

16. The water depths for the tests were 1 and 2 ft. The 2-ft depth was used more often, since for the same wave conditions, it allowed a wider range of relative depth values, d/L, than did the 1-ft depth. Ranges of test conditions are tabulated below, and are believed to approximate the conditions in which this type of structure can be used.

Depth d, ft	Period T, sec	Wavelength L, ft	Relative Depth, d/L	Wave Steepness H_i/L
1.0	1.0	4.53	0.22	0.02-0.08
	1.5	7.72	0.13	0.01-0.04
	2.0	10.76	0.09	0.01-0.05

(Continued)

Depth d, ft	Period T, sec	Wavelength L, ft	Relative Depth, d/L	H_i/L
2.0	0.75	2.88	0.69	0.01-0.09
	1.0	5.06	0.40	0.01-0.09
	1.5	9.84	0.20	0.01-0.09
	2.0	14.50	0.14	0.01-0.05
	2.5	18.70	0.11	0.01-0.03

Breakwater Sections Tested

Tire assembly

17. As mentioned earlier, the idea of a mobile breakwater made of used tires was developed and patented on the West Coast in 1964. The prototype Wave Maze, in use in Tomales Bay, California, was constructed to a finished assembly similar in appearance to that shown in fig. 7. This assembly, constructed in units with basic steps as shown in fig. 8, was fastened together as shown in fig. 9 and floated by means of a flotation material inside the tires (also shown in fig. 9).

18. The Wave Maze tested in the model was constructed of 6-in.-diameter tires assembled in the same fashion as in the prototype with one exception, that being the method of fastening the tires together. In the prototype, fig. 9, the tires were fastened together by bolts; however, due to the size of the model tires it was found difficult to follow this procedure in the model. Therefore, wire connections around the tires at their points of contact were employed instead of bolts. It is not known to what degree this method of connecting differs from the prototype method, but it is believed to allow comparable flexing of the assembly.

19. The flotation system used in the prototype was reproduced in the model by use of commercial styrofoam cut to the shape of the inside of the model tires and placed therein. Floating height of the test structure was varied by using flotation material in all the tires or any number of tires as desired. The manner in which the tires were assembled remained the same throughout the tests; therefore, the porosity of the model Wave Maze was the same for all the test structures and was found to be

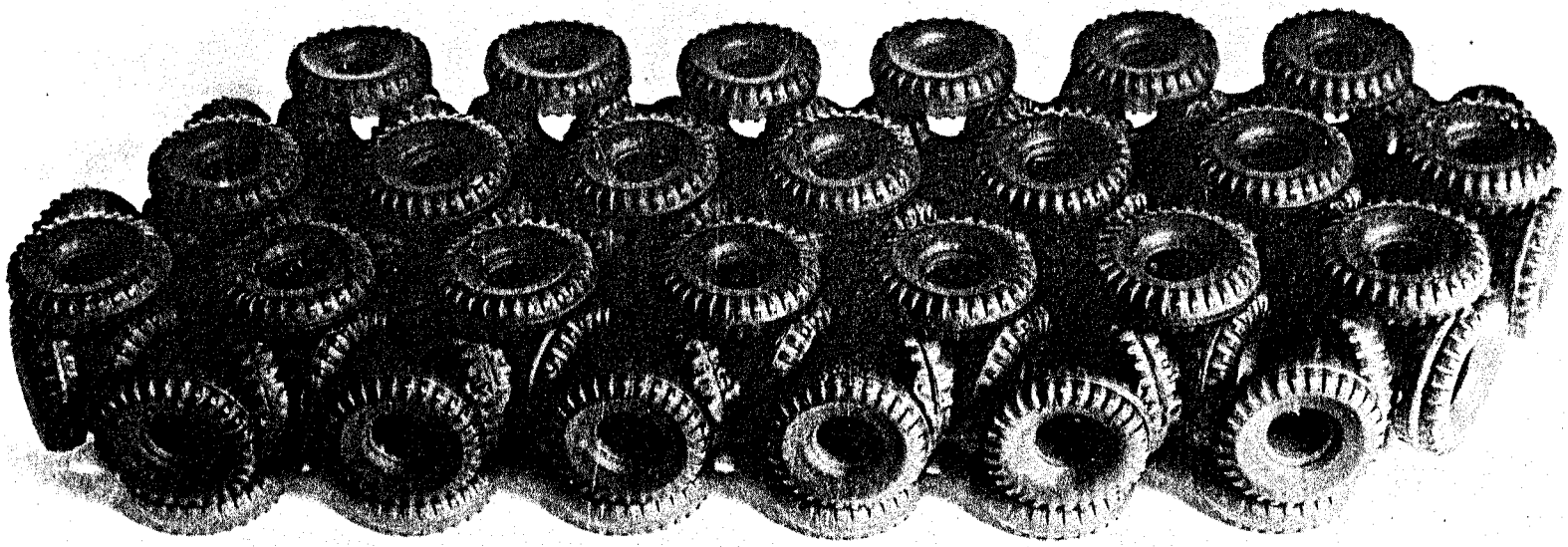

Fig. 7. Typical view of Wave Maze (from Stitt, reference 12)

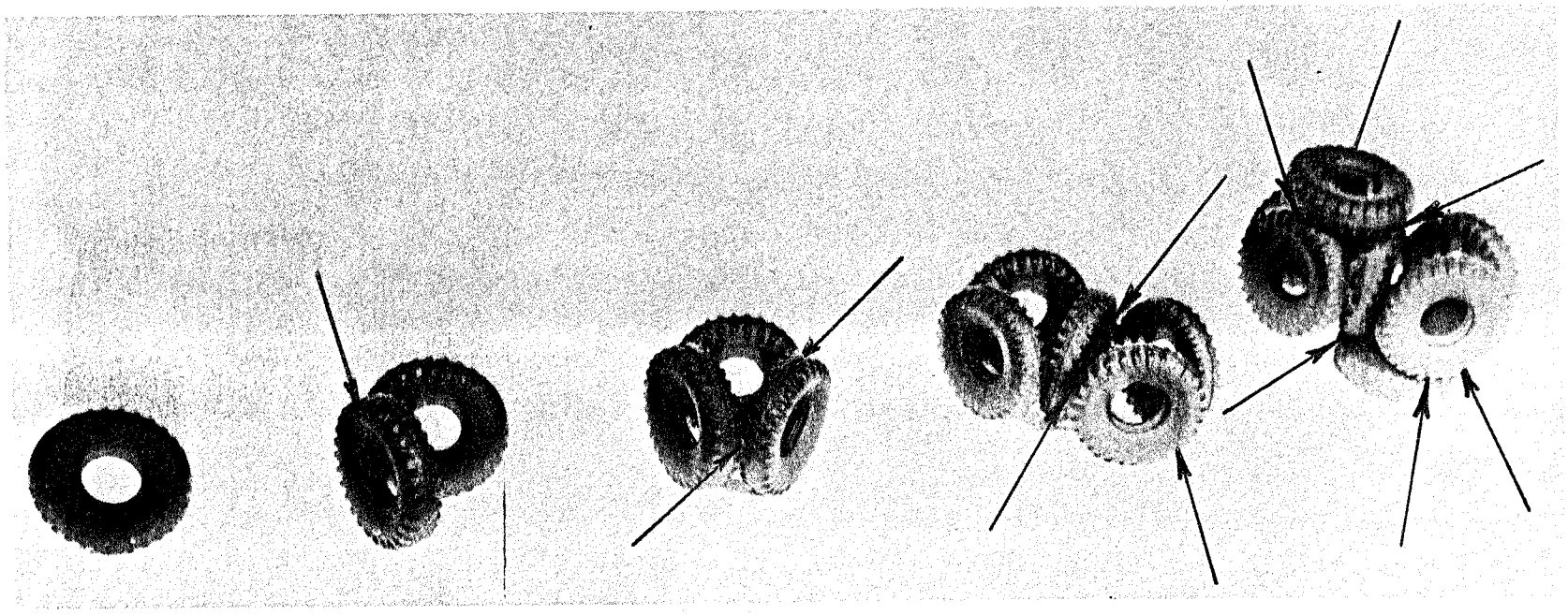

Fig. 8. Basic steps in the formation of the Wave Maze assembly (from Stitt, reference 12)

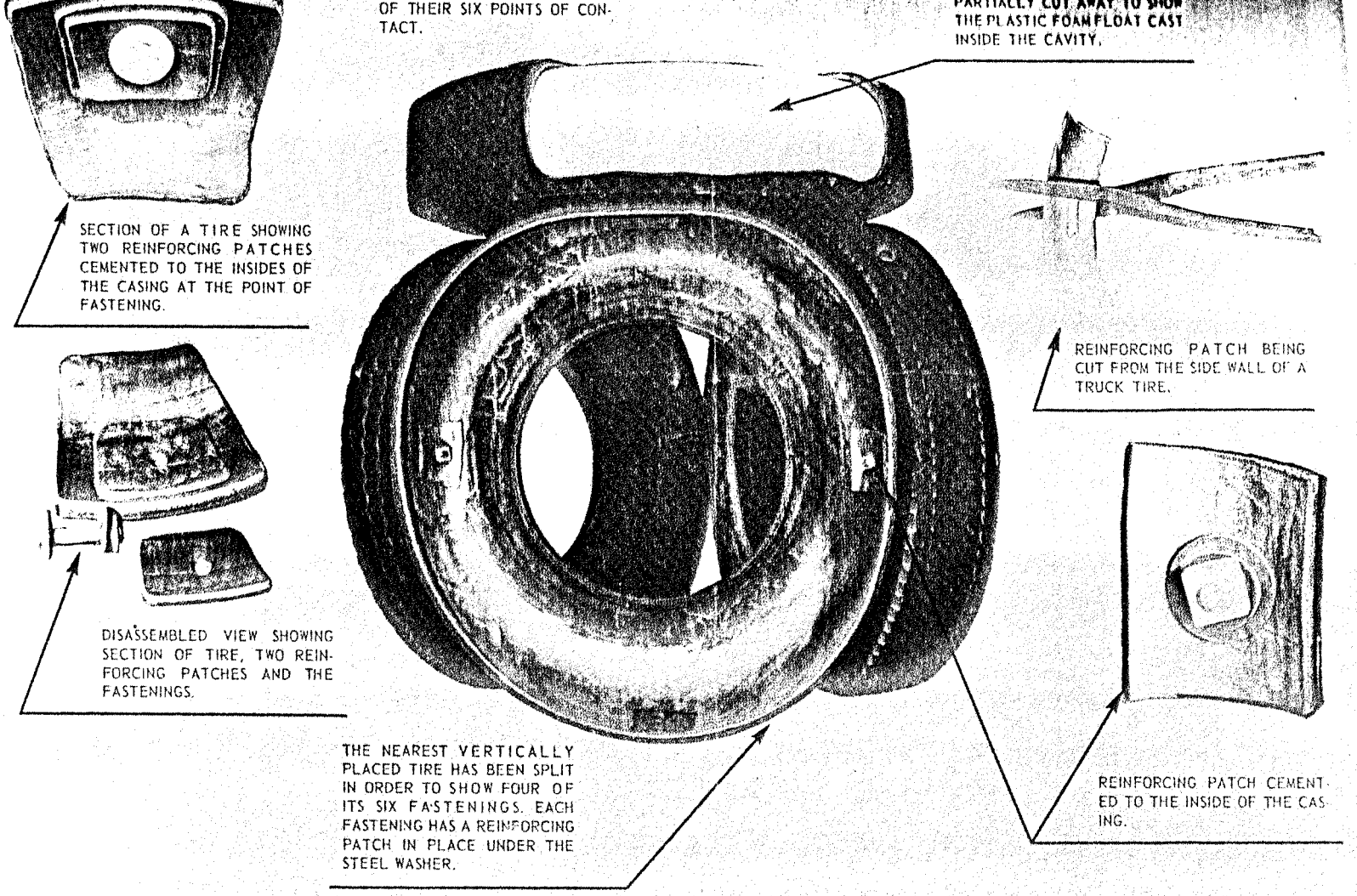

Fig. 9. Illustration of the Wave Maze connection and flotation system (from Stitt, reference 12)

about 60 percent. Fig. 10 shows the model Wave Maze under wave attack.

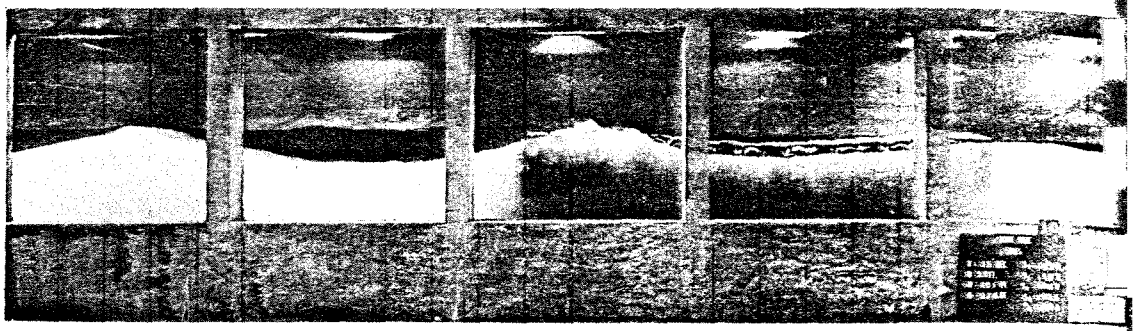

Fig. 10. Model Wave Maze under wave attack

20. Dimensions of tire assemblies tested are tabulated below:

Depth d, ft	Length (Sea to Shore Dimension) w, ft	Depth of Structure Below swl y, ft	Height of Structure Above swl h, ft	Width b_1, ft
1.0	2.33	0.50	0.22	1.88
2.0	2.33	0.50	0.22	1.88
1.0	5.45	0.50	0.22	1.88
2.0	5.45	0.50	0.22	1.88
2.0	10.15	0.50	0.22	1.88
2.0	10.15	0.98	0.32	1.88
2.0	10.15	1.12	0.18	1.88

Sphere assembly

21. The idea of a mobile breakwater made of spheres was developed the Waterways Experiment Station mainly for comparison purposes and since rubber balls were available from a previous study. To the author's knowledge, no prototype structure or model test data on an assembly made of spheres exist; however, it is believed that with model fabrication and construction methods, such a structure is practical.

22. The assembly of spheres tested in the model was constructed of 5-inch-diameter rubber balls assembled as shown in fig. 11. This was the only pattern for which the balls were tested, and the porosity was found to be about 57 percent. The top floating layer of balls utilized metal bands with small hooks as shown in fig. 11 to connect to each other and to the lower layer of balls. Connection of the lower balls was obtained by means of a nylon cord system. Holes cut in the lower balls allowed them to fill with water, keep their original shape, and remain submerged. The

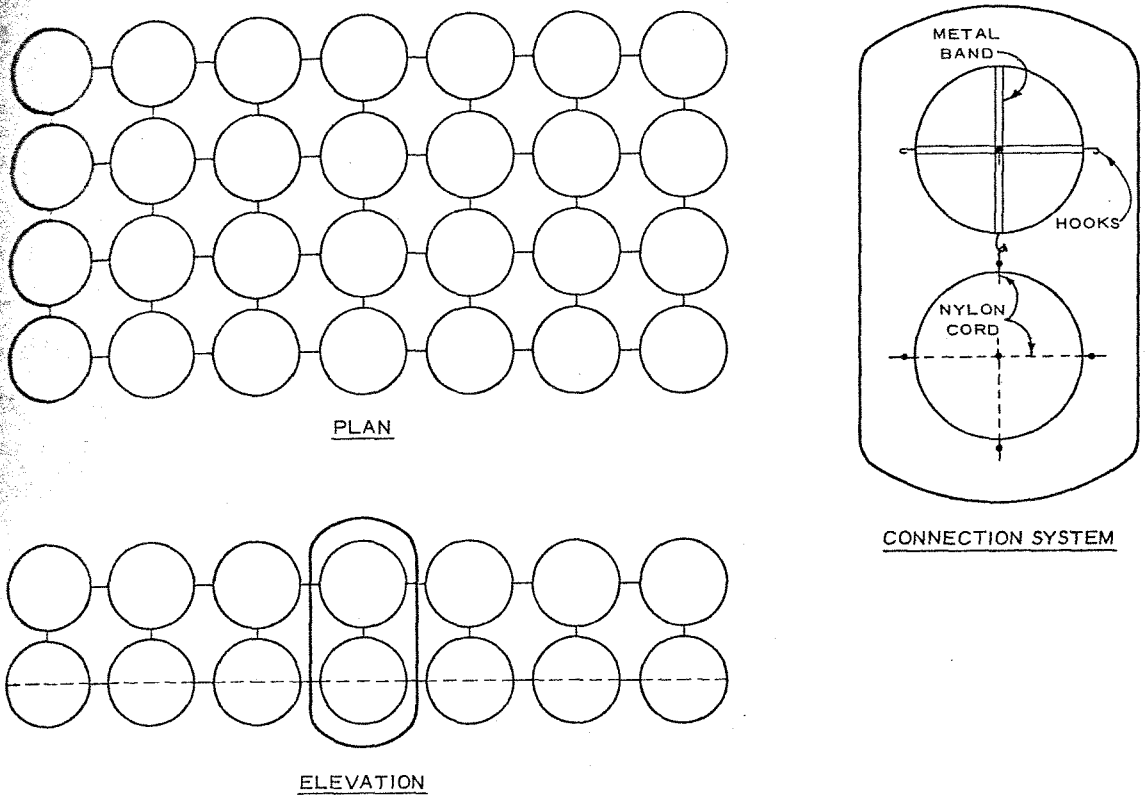

Fig. 11. Sphere assembly and connection system

overall responses of the tire and sphere assemblies to wave action were the same with the exception that the connections used for the spheres were more flexible than those of the tires. This flexibility allowed the spheres to flex more with the waves, causing a jerking motion between the individual units as the waves progressed the length of the assembly. Fig. 12 shows the model sphere assembly being subjected to wave action.

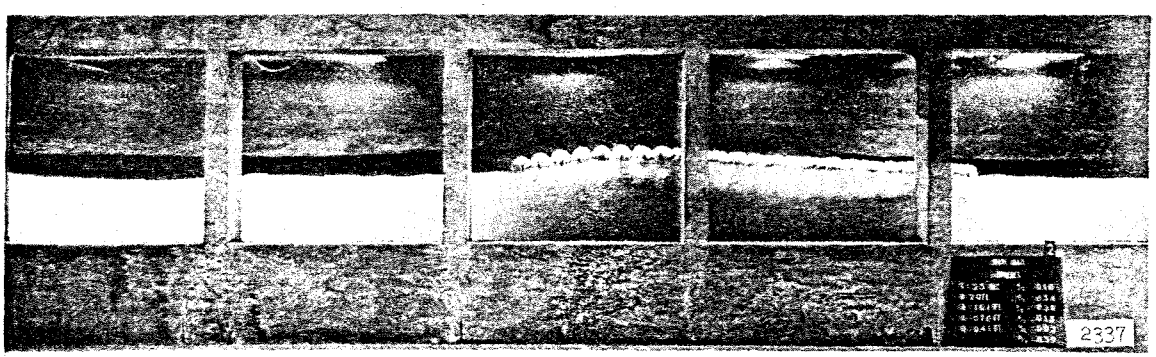

Fig. 12. Model sphere assembly under wave attack

23. Dimensions of sphere assemblies tested are tabulated below:

Depth d, ft	Length (Sea to Shore Dimension) w, ft	Depth of Structure Below swl y, ft	Height of Structure Above swl h, ft	Width b_1, ft
1.0	2.55	0.60	0.26	1.83
2.0	2.55	0.60	0.26	1.83
1.0	6.00	0.60	0.26	1.83
2.0	6.00	0.60	0.26	1.83
2.0	10.00	0.60	0.26	1.83

PART IV: ANALYSIS OF TEST RESULTS

24. To be effective, a floating breakwater must extend deep enough into the water that little wave power can be transmitted beneath it, and it must have the mass and damping characteristics necessary to prevent it from moving extensively so it will not transmit wave power as if it were a portion of the water. In order to fulfill the latter requirement, the floating breakwater must have natural periods that are large compared with the wave periods to which it will be subjected. This means that its mass should be large, its viscous and form damping large, and its elasticity small. Its elasticity is represented by its change in buoyancy as it heaves, rolls, and pitches. In order to make the elasticity small and the mass large at the same time, the bulk of the breakwater must be below the water surface at all times.[13]

25. The experimental results for the breakwater sections tested are given in tables 1 and 2. Table 1 gives the incident, reflected, and transmitted wave data for the tire and sphere assemblies, and table 2 gives the mooring line force measurements for the two assemblies. From the data given in table 1, the coefficient of reflection K_r, coefficient of transmission K_t, and the ratio of the power dissipated by the breakwater to the wave power P_D/P were calculated using equations 10, 11, and 14, respectively, and are presented in table 3. The wavelength L in this table was computed knowing the water depth and using the relation

$$L = \frac{gT^2}{2\pi} \tanh kd \qquad (24)$$

The ratios w/L, d/L, y/d, h/d, and H_i/L were computed directly from the test data given in table 1. From the data given in table 2, the ratios between the maximum force in the mooring lines per unit area of breakwater cross section perpendicular to direction of wave propagation, f_c, to the maximum theoretical horizontal force exerted on a total reflecting vertical wall per unit area of flow cross section perpendicular to the direction of wave propagation, $f_{t_{max}}$, were calculated and are presented in table 4. The wavelength L in this table was computed using

tion 21.

26. The results listed in tables 3 and 4 are also presented graphically as follows:

a. Effect of h/d, y/d, and H_i/L on K_r, tire assembly (plates 3-5).

b. Effect of h/d, y/d, and H_i/L on K_t, tire assembly (plates 6-8).

c. Variation of K_r with H_i/L for different values of w/L and y/d, tire and sphere assemblies (plates 9-12).

d. Variation of K_t with H_i/L for different values of w/L and y/d, tire and sphere assemblies (plates 13-16).

e. Variation of P_D/P with H_i/L for different values of w/L and y/d, tire and sphere assemblies (plates 17-20).

f. Variation of $f_c/f_{t_{max}}$ with w/L, tire and sphere assemblies (plates 22-23).

Though the graphical presentations are placed in the order given above for the sake of recording the results, it must be kept in mind that in the final appraisal these results cannot be considered separately but must be viewed integrally with respect to their interrelations.

27. The experimental data plotted in the above-referenced plates exhibit considerable scatter. However, results from tests under the same conditions were fairly reproducible. Most of the scatter can be attributed to the complex flow processes involved which make the number of parameters chosen to correlate the data inadequate to account for all the physical factors present. Part of the scatter, however, is attributed to the rounded off values of H_i/L, w/L, and y/d used in the plots. This was done for convenience in presenting the data graphically. Other factors that caused scatter of the test results are experimental inaccuracies such as:

a. Using a fixed wave rod to measure the height of the transmitted wave, thus assuming that the wave reflection from

the absorber beach shoreward of the test structure is negligible. This may result in some error in the values of the transmitted wave heights measured.

b. Mooring the breakwater on the sea-side end only during some of the tests. This caused the breakwater to ride the wave form, resulting in a decrease in its efficiency.

c. The occurrence of transverse oscillations in the wave flume due to resonance.

Due to the considerable scatter in the experimental data plotted, in most of the plates no attempt was made to draw curves showing the trend of the data.

Effect of h/d , y/d , and H_i/L on Reflection and Transmission Coefficients, Tire Assembly

Reflection coefficient

28. No attempt is made in this report to present the variation of reflection or transmission coefficients with w/L and h/d for the sphere assembly because of the limited number of tests conducted for that assembly. However, it is believed that relations similar to those obtained for the tire assembly are to be expected for the sphere assembly.

29. Results of tests on the effect of h/d , the relative height of the breakwater above swl, on the value of the wave reflection coefficient, K_r , for the tire assembly are presented in plate 3. This plate shows the variation of K_r with w/L and with h/d for different values of H_i/L and for $y/d \approx 0.50$. It can be seen that, contrary to expectations, a change in h/d , keeping the values of H_i/L , w/L , and y/d constant, does not seem to affect the value of K_r . In other words, the height to which the breakwater extends above the water surface does not seem to affect the value of the wave reflection coefficient of the tire assembly breakwater. This is believed to result from the riding of the breakwater with the wave form. Plate 3 does indicate, however, an increase in K_r for increasing values of w/L .

30. Results of tests on the effect of y/d , the relative depth of the breakwater below swl, on the value of K_r for the tire assembly are

presented in plate 4 as the variation of K_r with w/L and with y/d for different values of H_i/L . This plate shows that for constant values of H_i/L and w/L , K_r is slightly larger for tests with $y/d \approx 0.50$ than for tests with $y/d = 0.25$. Like plate 3, plate 4 indicates an increase in K_r for increasing values of w/L .

31. Results of tests on the effect of the wave steepness H_i/L on the value of K_r for the tire assembly are presented in plate 5 as the variation of K_r with w/L and with H_i/L for $y/d \approx 0.50$. The wave steepness used varied from 0.01 to 0.08. Despite the scatter in the experimental data plotted in plate 5, the general trend of the data indicates that K_r decreases for increasing values of H_i/L and that K_r increases for increasing values of w/L .

Transmission coefficient

32. Results of tests on the effect of h/d on the value of the wave transmission coefficient, K_t , for the tire assembly are presented in plate 6 as the variation of K_t with w/L and with h/d for different values of H_i/L and for $y/d \approx 0.50$. It can be seen that, contrary to expectation, a change in h/d , keeping constant the values of H_i/L , w/L , and y/d , does not seem to affect the value of K_t . Again, as mentioned in paragraph 29, this is believed to result from the riding of the breakwater with the wave form. Plate 6 does show, however, that K_t decreases for increasing values of w/L .

33. Results of tests on the effect of y/d on K_t for the tire assembly are presented in plate 7 as the variation of K_t with w/L and with y/d for different values of H_i/L . The plot shows that for constant values of H_i/L and w/L , K_t decreases slightly for increasing values of y/d . Like plate 6, plate 7 indicates that K_t decreases for increasing values of w/L .

34. Results of tests on the effect of H_i/L on the value of K_t for the tire assembly are presented in plate 8 as the variation of K_t with w/L and with H_i/L for $y/d \approx 0.50$. The wave steepnesses used varied from 0.01 to 0.09. It can be seen that K_t decreases for increasing values of H_i/L and for increasing values of w/L .

Summary of results

35. The analysis of test data presented above indicates that:

a. The relative height of the breakwater above swl has no significant effect on the values of the reflection and transmission coefficients. This is contrary to expectation and is believed to have been caused by the high flexibility which caused the breakwater to follow the wave form.

b. Increasing the relative depth of the breakwater below swl resulted in a slight increase and a slight decrease in the reflection and transmission coefficients, respectively. Although the values of y/d used were 0.25 and about 0.50, i.e., a hundred percent increase, the resulting variation in the values of K_r and K_t was small. This might be expected for waves having small steepness; however, for waves having a large steepness, a larger variation (than that recorded) in the values of K_r and K_t for the two values of y/d used might be expected but was not obtained because of the high flexibility of the breakwater.

c. An increase in the relative length of the breakwater, w/L, resulted in an increase and decrease in the reflection and transmission coefficients, respectively.

d. The wave steepness has a more pronounced effect than h/d or y/d on the reflection and transmission coefficients. The graphical presentation of the effect of H_i/L on K_r, K_t, and P_D/P can be shown more conveniently by plotting K_r, K_t, and P_D/P versus H_i/L instead of w/L as shown in plates 9-20.

Variation of Reflection Coefficient with H_i/L for Different Values of w/L and y/d, Tire and Sphere Assemblies

Tire assembly

36. Plates 9 and 10 show the relation between K_r and H_i/L for different values of w/L and for $y/d \approx 0.50$ and 0.25, respectively. It can be seen from plate 9 that:

a. For w/L values of 3.9 to 2.0, 1.1 to 0.6, and 0.25, the average value of K_r for the range of wave steepnesses used was about 0.4, 0.2, and 0.1, respectively. This indicates that increasing the relative length of the breakwater about 300 or 400 percent will result in only doubling the value of the wave reflection coefficient.

b. K_r decreases for increasing values of H_i/L ; however, the value of K_r does not seem to be as sensitive to changes in H_i/L as it is to changes in w/L .

c. In order for the tire assembly type of breakwater to be effective, the length of the breakwater should be on the order of one-half to one wavelength.

The effect of y/d on K_r can be seen by comparing plates 9 and 10. It can be seen in these plots that for w/L values of 0.2 to 1.1, K_r was about 0.2 and 0.1 for y/d values of 0.50 and 0.25, respectively.

Sphere assembly

37. Plates 11 and 12 show the relation between K_r and H_i/L for different values of w/L and for $y/d = 0.3$ and 0.6 , respectively. The data are scattered and do not follow a definite trend, but indicate an average value of about 0.2 for K_r . However, the two plots show that for comparable values of H_i/L , w/L , and y/d , the reflection coefficient for the sphere assembly was slightly larger than that for the tire assembly. This is believed to be due to the low porosity, e , of the sphere assembly, which was about 0.57 as compared to about 0.8 for the tire assembly.

Variation of Transmission Coefficient with H_i/L for Different Values of w/L and y/d , Tire and Sphere Assemblies

Tire assembly

38. Plates 13 and 14 show the relation between K_t and H_i/L for different values of w/L and for $y/d \approx 0.50$ and 0.25, respectively. It can be seen from plate 13 that:

a. K_t decreases for increasing values of w/L . This decrease is sharp for $w/L \leq 2.0$.

b. K_t decreases for increasing values of H_i/L . This decrease is sharp for $H_i/L \leq 0.04$.

c. For the tire assembly type of breakwater to be effective, the length of the breakwater should be on the order of one-half to one wavelength and the wave steepness $\geq$ about 0.04.

The effect of y/d on K_t can be seen by comparing plates 13 and 14. It can be seen in these plots that for w/L values of 0.45 to 1.1, K_t was about 30 percent smaller for $y/d \approx 0.50$ than for $y/d = 0.25$.

Sphere assembly

39. Plates 15 and 16 show the relation between K_t and H_i/L for different values of w/L and for $y/d = 0.3$ and 0.6 , respectively. It can be seen from plate 15 that:

a. K_t decreases for increasing values of w/L .

b. K_t decreases for increasing values of H_i/L .

c. In order for this sphere assembly type of breakwater to be effective, the length of the breakwater should be on the order of one-half to one wavelength and the wave steepness $\geq$ about 0.04.

A comparison of the data shown in plates 15 and 16 indicates that changing y/d values from 0.3 to 0.6 does not seem to have a significant effect on the value of K_t . The experimental data shown in plates 13-16 indicate that for comparable values of H_i/L , w/L , and y/d , the transmission coefficient for the sphere assembly was slightly smaller than that for the tire assembly. As mentioned in paragraph 37, this is believed to be due to the low porosity of the sphere assembly, which was about 0.57 as compared to about 0.8 for the tire assembly.

Variation of Power Dissipated by Breakwater with H_i/L for Different Values of w/L and y/d , Tire and Sphere Assemblies

40. The wave power dissipated by the breakwater was determined from equation 14. This equation reflects the combined trend of reflection and

transmission coefficients obtained for the breakwater assemblies tested. In connection with trends of power dissipated, presented in plates 17-20, it is important to observe the variation of wave power transmission as a function of the wave parameter kd as shown in plate 21. This plot shows that down to $z/d \approx -0.4$, over two-thirds of the wave power is concentrated within that depth for all values of $kd > 1.5$. This explains the effectiveness of the breakwaters relative to wavelength and the marked reduction in the efficiency of the breakwaters with increasing wavelength.

Tire assembly

41. Plates 17 and 18 show the relation between P_D/P and H_i/L for different values of w/L and for $y/d \approx 0.50$ and 0.25, respectively. It can be seen from plate 17 that:

a. Power dissipated increases for increasing wave steepness. The increase is sharp for $H_i/L \leq$ about 0.05.

b. Power dissipated increases for increasing relative length of the breakwater, w/L. The increase is sharp for $w/L \leq$ about 1.0. This indicates, as mentioned earlier, that in order for the tire assembly type of breakwater to be effective, the length of the breakwater should be on the order of one-half to one wavelength and the wave steepness $\geq$ about 0.04.

A comparison of the data shown in plates 17 and 18 indicates that changing y/d values from 0.50 to 0.25 resulted in an average decrease of about 40 percent in the power dissipated.

Sphere assembly

42. Plates 19 and 20 show the relation between P_D/P and H_i/L for different values of w/L and for $y/d = 0.3$ and 0.6, respectively. It can be seen from plate 19 that:

a. Power dissipated increases for increasing wave steepness.

b. Power dissipated increases for increasing relative length of the breakwater.

A comparison of the data shown in plates 19 and 20 indicates that changing y/d from 0.3 to 0.6 resulted in an increase in the power dissipated; however, because of the limited number of tests conducted for the sphere

assembly and the considerable scatter in the test data shown in plate 20, it is not feasible to predict the percentage increase in the power dissipated by the breakwater as a result of this increase in relative depth. The experimental data shown in plates 18 and 19 indicate that for comparable values of H_i/L , w/L , and y/d , the power dissipated by the sphere assembly was larger than that dissipated by the tire assembly. As mentioned earlier, this is believed to be due to the low porosity of the sphere assembly which was about 0.57 as compared to about 0.8 for the tire assembly.

Variation of Force in Mooring Lines with w/L , Tire and Sphere Assemblies

43. The total forces exerted on the mooring lines of the breakwater were related to the maximum total horizontal force exerted on a vertical reflecting wall as computed from equation 21. The slope of the mooring line was arbitrarily selected to be 1:3 (1 vertical and 3 horizontal). The recorded mooring forces were corrected to account for the fact that as the wave period approached the natural period of the breakwater system, the indicated force was greater than the force actually experienced by the breakwater.

44. The variation in the ratio of the maximum force in the breakwater mooring lines to the maximum total horizontal force exerted on a vertical reflecting wall, $f_c/f_{t_{max}}$, with w/L is shown in plates 22 and 23 for the tire and sphere assemblies, respectively. It can be seen from these plots that:

a. The forces on the breakwater mooring lines, f_c , are relatively small compared to the force due to total reflection of a vertical wall, $f_{t_{max}}$. For the tire assembly, $f_c/f_{t_{max}}$ did not exceed 0.29 and 0.22 for the seaward and shoreward mooring lines, respectively. For the sphere assembly, $f_c/f_{t_{max}}$ did not exceed 0.47 and 0.16 for the seaward and shoreward mooring lines, respectively.

b. The forces in the seaward mooring lines are considerably larger than those in the shoreward mooring lines.

subject to large drift if slack in the mooring lines is large.

c. The forces in the mooring lines of the sphere assembly were higher than the forces in the mooring lines of the tire assembly. This is believed to be due to the smaller porosity of the sphere assembly, which was about 0.57 as compared to about 0.8 for the tire assembly.

PART V: CONCLUSIONS

45. The following general conclusions are drawn:

a. For the tire assembly, the relative height to which the breakwater extends above still-water level, h/d, does not seem to affect the wave reflection coefficient K_r or the wave transmission coefficient K_t. This is contrary to expectation and is due to the high flexibility of the breakwater, which caused it to move extensively as if it were a portion of the water. An increase in y/d resulted in a slight decrease in the coefficient of wave transmission, K_t. No attempt was made in this study to determine the effects of h/d on K_r and K_t for the sphere assembly. However, it is believed that results similar to those obtained for the tire assembly can be expected.

b. For the tire and sphere assemblies, an increase in the relative length of the breakwater, w/L, caused an increase in K_r. For the tire assembly, increasing the value of w/L about 300 or 400 percent resulted in only doubling the value of K_r.

c. An increase in the wave steepness, H_i/L, caused a decrease in K_r for the tire and sphere assemblies. However, the value of K_r does not seem to be as sensitive to changes in H_i/L as it is to changes in w/L.

d. For the tire and sphere assemblies, an increase in w/L caused a decrease in K_t. For the tire assembly, the decrease was sharp for $w/L \leq 2.0$.

e. An increase in H_i/L caused a decrease in K_t for the tire and sphere assemblies. For the tire assembly, the decrease was sharp for $H_i/L \leq 0.04$.

f. For the tire and sphere assemblies, an increase in H_i/L and w/L caused an increase in the power dissipated by the breakwater, P_D/P. For the tire assembly, the increase was sharp for $H_i/L \leq$ about 0.05 and $w/L \leq$ about 1.0.

tively small compared to the force due to total reflection of a vertical wall, $f_{t_{max}}$. For the tire assembly, $f_c/f_{t_{max}}$ did not exceed 0.29 and 0.22 for the seaward and shoreward mooring lines, respectively. For the sphere assembly, $f_c/f_{t_{max}}$ did not exceed 0.47 and 0.16 for the seaward and shoreward mooring lines, respectively.

h. The forces in the seaward mooring lines are considerably larger than those in the shoreward mooring lines. Consequently, these types of floating breakwaters will be subject to large drift.

i. For the tire and sphere assemblies, an increase in the relative depth of the breakwater below still-water level, y/d, caused an increase in K_r, P_D/P, and $f_c/f_{t_{max}}$ and a decrease in K_t.

j. The sphere assembly has larger values of K_r, P_D/P, and $f_c/f_{t_{max}}$ and a smaller value of K_t than the tire assembly. This is caused by the low porosity, e, of the sphere assembly which was about 0.57 as compared to about 0.8 for the tire assembly.

k. Finally, it is believed that in order for these types of floating breakwaters to be ~~effective~~ efficient, their length should be on the order of one-half to one wavelength, their depth on the order of half the water depth, and the wave steepness equal to or greater than about 0.04. The effectiveness of these breakwaters can be improved by decreasing their porosity and flexibility; however, this would cause an increase in the mooring forces and the drift.

1. Ippen, A. T. and Goda, Yoshimi, "Wave Induced Oscillations in Harbors: The Solution for a Rectangular Harbor Connected to the Open-Sea," Report No. 59, Aug 1963, Massachusetts Institute of Technology, Hydrodynamics Laboratory, Cambridge, Mass.

2. Ippen, A. T. and Goda, Yoshimi, "Wave Induced Oscillations in Harbors: The Solution for a Rectangular Harbor with Partially Open Boundary," Report No. 69, June 1963, Massachusetts Institute of Technology, Hydrodynamics Laboratory, Cambridge, Mass.

3. Ippen, A. T. and Goda, Yoshimi, "Wave Induced Oscillations in Harbors: The Solution for a Rectangular Harbor with Partially Open-Tube Systems," Report No. 73, July 1964, Massachusetts Institute of Technology, Hydrodynamics Laboratory, Cambridge, Mass.

2. Carr, J. H., "Mobile Breakwater," Proceedings, Second Conference on Coastal Engineering, Houston, Nov 1951, pp 281-295.

3. Skerrett, R. G., "Smashing Angry Seas with Bubbles of Compressed Air," Compressed Air Magazine, Vol 26, No. 1, Jan 1921, pp 9921-9927.

4. Hudson, R. Y., "Model Tests of Portable Breakwaters for D-Day Invasion Harbors," Civil Engineering, Vol 15, Jan-Dec 1945, pp 405-408.

5. Lochner, R., Faber, O., and Penney, W. G., "The 'Bombardon' Floating Breakwater," The Civil Engineer in War, Institution of Civil Engineers, Vol 2, 1948, pp 256-290.

6. Evans, J. T., "Pneumatic and Similar Breakwaters; Model Experiment Using Surface Currents," Dock and Harbour Authority, Vol 36, No. 422, Dec 1955, pp 251-256.

7. Straub, L. G., Herbich, J. B., and Bowers, C. E., "An Experimental Study of Hydraulic Breakwaters," Proceedings, Sixth Conference on Coastal Engineering, Gainesville, 1957, pp 715-728.

8. Frederiksen, H. D. and Wetzel, J. M., "An Exploratory Investigation of Mobile Breakwaters," Project Report No. 60, June 1959, University of Minnesota, St. Anthony Falls Hydraulic Laboratory, St. Paul, Minn.

9. Ripkin, J. F., "An Experimental Study of Flexible Floating Breakwaters," Technical Paper No. 31, Series B, Oct 1960, University of Minnesota, St. Anthony Falls Hydraulic Laboratory, St. Paul, Minn.

10. Wiegel, R. L., Shen, H. W., and Cumming, J. D., "Final Report on Hovering Breakwater," Technical Report, Series 140, Issue 5, June 1961, University of California, Hydraulic Engineering Laboratory, Berkeley, Calif.

11. Bulson, P. S., "Transportable Breakwaters; a Feasibility Study," Military Engineering Experimental Establishment Report Res. 42.1/4, April 1964, Christchurch, Hampshire, England.

12. Stitt, R. L., Wave Maze, Temple City, Calif., 1963.

13. Wiegel, R. L., Oceanographic Engineering, Prentice-Hall, Inc., Englewood Cliffs, N. J., 1964.

Table 1

Test Results, Wave Measurements for Tire and Sphere Assemblies

Test No.	Water Temp °F	d, ft	y, ft	h, ft	w, ft	T, sec	$H_i = 2a_1$ ft	$H_r = 2a_2$ ft	$H_t = 2a_3$ ft
					Tire Assembly				
1	58	2.0	1.12	0.18	10.15	0.75	--	--	--
2							--	--	--
3							0.07	0.02	0.01
4							--	--	--
5							0.02	0.01	0.01
6						1.0	0.04	0.01	0.02
7							0.14	0.06	0.03
8							0.19	0.06	0.04
9							--	--	--
10							--	--	--
11						1.5	0.14	0.02	0.10
12							0.30	0.06	0.19
13							0.40	0.06	0.21
14							0.67	0.13	0.27
15							0.74	0.12	0.29
16						2.0	0.17	0.02	0.14
17							0.42	0.06	0.23
18							0.73	0.33	0.27
19							0.85	0.22	0.31
20						2.5	0.21	0.07	0.21
21							0.87	0.25	0.35
22							0.76	0.34	0.40
23	49	1.0	0.50	0.22	5.45	1.0	0.10	0.02	0.06
24							0.18	0.02	0.09
25							0.27	0.03	0.12
26							0.35	0.07	0.14
27						1.5	0.09	0.01	0.08
28							0.14	0.04	0.13
29							0.23	0.03	0.17
30							0.30	0.04	0.19
31						2.0	0.10	0.03	0.10
32							0.21	0.04	0.18
33							0.32	0.05	0.24
34							0.41	0.08	0.28
35	50	2.0				1.0	--	--	--
36							--	--	--
37							--	--	--
38							--	--	--
39						1.5	0.21	0.05	0.20
40							0.31	0.05	0.26
41							0.45	0.08	0.29
42							0.51	0.07	0.34
43							0.47	0.09	0.39
44							0.73	0.12	0.53
45							--	--	--

(Continued)

Test No.	Water Temp °F	d, ft	y, ft	h, ft	w, ft	T, sec	$H_i = 2a_1$ ft	$H_r = 2a_2$ ft	H
					Tire Assembly (Continued)				
46	50	2.0	0.50	0.22	5.45	2.0	0.26	0.04	
47							0.33	0.02	
48							0.42	0.03	
49							0.53	0.03	
50							0.60	0.05	
51							0.68	0.13	
52							0.79	0.09	
53		1.0			2.33	1.0	--	--	
54							0.19	0.05	
55							0.29	0.07	
56							0.30	0.07	
57						1.5	0.11	0.01	
58							0.20	0.02	
59							0.27	0.02	
60							--	--	
61						2.0	0.10	0.01	
62							0.17	0.03	
63							0.24	0.04	
64							0.32	0.06	
65	49	2.0				1.0	--	--	
66							--	--	
67							--	--	
68							--	--	
69						1.5	0.24	0.03	
70							0.29	0.02	
71							0.39	0.05	
72							0.47	0.05	
73							0.50	0.07	
74							0.68	0.09	
75	50					2.0	0.26	0.04	
76							0.34	0.04	
77							0.44	0.08	
78							0.54	0.06	
79							0.64	0.07	
80							0.74	0.05	
81							0.81	0.09	
82	62		0.98	0.32	10.15	0.75	--	--	
83							0.02	0.01	
84							--	--	
85							0.11	0.05	
86							--	--	
87						1.5	0.13	0.03	
88							0.22	0.05	
89							0.41	0.11	
90							0.62	0.12	
91							0.71	0.11	

Table 1 (Concluded)

Test No.	Water Temp °F	d, ft	y, ft	h, ft	w, ft	T, sec	$H_i = 2a_1$ ft	$H_r = 2a_2$ ft	$H_t = 2a_3$ ft
				Tire Assembly (Continued)					
92	62	2.0	0.98	0.32	10.15	2.5	0.26	0.07	0.22
93	↓						0.73	0.17	0.38
94							0.82	0.21	0.42
95	65		0.50	0.22		1.5	0.11	0.03	0.13
96							0.27	0.05	0.21
97							0.42	0.06	0.28
98							0.68	0.07	0.35
99							0.73	0.09	0.35
				Sphere Assembly					
1	51	1.0	0.60	0.26	2.55	1.0	0.09	0.02	0.02
2							0.22	0.03	0.06
3							0.27	0.09	0.10
4							0.24	0.10	0.10
5						1.5	0.14	--	0.09
6							0.21	0.05	0.16
7							0.31	0.07	0.22
8							0.39	0.09	0.33
9						2.0	0.11	0.02	0.10
10							0.17	0.02	0.16
11							0.25	0.05	0.22
12							0.34	0.08	0.31
13		2.0				1.0	0.09	0.03	0.03
14							--	--	--
15							--	--	--
16							--	--	--
17						1.5	0.25	0.02	0.21
18							0.32	0.08	0.25
19							0.34	0.04	0.31
20							0.49	0.02	0.37
21							--	--	--
22							--	--	--
23							--	--	--
24						2.0	0.24	0.03	0.25
25							0.34	0.07	0.31
26							0.44	0.12	0.43
27							0.52	0.14	0.53
28							0.62	0.08	0.62
29							0.71	0.08	0.73
30							0.82	0.10	0.76
31	50	1.0			6.00	1.0	0.09	0.02	0.02
32							0.19	0.03	0.07
33							0.24	0.04	0.09
34							0.29	0.11	0.10
35						1.5	0.11	0.03	0.07
36							0.16	0.06	0.11
37							0.31	0.07	0.16
38							0.33	0.05	0.20

Test No.	Water Temp °F	d, ft	y, ft	h, ft	w, ft	T, sec	$H_i = 2a_1$ ft	$H_r = 2a_2$ ft	$H_t = 2a_3$ ft
				Sphere Assembly (Continued)					
39	50	1.0	0.60	0.26	6.00	2.0	0.13	0.04	0.11
40							0.24	0.01	0.19
41							0.33	0.06	0.25
42							0.42	0.16	0.32
43	49	2.0				1.0	--	--	--
44							--	--	--
45							--	--	--
46							--	--	--
47						1.5	0.28	0.05	0.18
48							0.30	0.09	0.21
49							0.36	0.09	0.26
50							0.45	0.13	0.30
51	50						0.55	0.17	0.33
52							--	--	--
53							--	--	--
54						2.0	0.22	0.03	0.19
55							0.30	0.04	0.23
56							0.39	0.04	0.27
57							0.50	0.05	0.33
58							0.58	0.12	0.40
59							0.66	0.10	0.29
60							--	--	--
61	67				10.00	0.75	0.03	0.01	0.01
62							--	--	--
63							0.07	0.01	0.01
64							--	--	--
65							--	--	--
66						1.0	0.02	0.01	0.01
67							0.11	0.02	0.02
68							0.19	0.07	0.02
69							--	--	--
70							--	--	--
71						1.5	0.09	0.03	0.08
72							0.27	0.07	0.20
73							0.34	0.02	0.24
74	68						0.64	0.14	0.32
75							0.71	0.13	0.36
76						2.0	0.15	0.07	0.18
77							0.33	0.09	0.29
78							0.61	0.10	0.42
79							0.72	0.14	0.44
80						2.5	0.24	0.05	0.23
81							0.70	0.11	0.51
82							0.86	0.18	0.56

Table 2

Mooring Line Force Measurements, Tire and Sphere Assemblies

Test No.	d, ft	y, ft	h, ft	w, ft	T, sec	$H_i = 2a_1$ ft	F_1, lb	F_2, lb
				Tire Assembly				
1	2.0	0.98	0.32	10.15	0.75	0.03	--	--
2						0.09	--	--
3						0.14	--	--
4						0.20	--	--
5						0.26	0.5	--
6					1.0	0.05	--	--
7						0.15	0.5	0.3
8						0.25	1.4	0.4
9						0.35	3.5	0.6
10						0.46	6.0	1.2
11					1.5	0.10	0.5	2.2
12						0.30	5.5	3.7
13						0.49	11.0	5.2
14						0.69	20.0	6.7
15						0.89	24.0	7.7
16					2.0	0.15	1.5	3.2
17						0.44	9.0	7.2
18						0.73	24.0	9.2
19						0.78	26.0	10.2
20					2.5	0.19	2.0	2.0
21						0.56	15.6	7.8
22						0.87	19.5	8.5
				Sphere Assembly				
1	2.0	0.60	0.26	10.00	0.75	0.01	--	--
2						0.04	--	--
3						0.07	--	--
4						0.14	0.3	--
5						0.23	1.5	0.2
6					1.00	0.02	--	--
7						0.11	0.5	0.2
8						0.19	1.5	0.3
9						0.14	4.0	0.6
10						0.42	5.5	1.0
11					1.50	0.09	0.5	1.0
12						0.27	2.8	1.8
13						0.34	7.5	3.2
14						0.64	19.0	6.8
15						0.71	22.0	7.2
16					2.00	0.21	1.0	2.7
17						0.33	3.0	2.5
18						0.61	7.5	5.5
19						0.72	15.0	7.5
20					2.50	0.21	1.0	2.7
21						0.67	7.5	4.0
22						0.75	9.0	4.5

Table 3

K_r, K_t, and P_D/P, Tire and Sphere Assemblies

Test No.	L, ft	w/L	d/L	y/d	h/d	H_i/L	K_r	K_t	P_D/P
					Tire Assembly				
1	2.88	3.53	0.69	0.56	0.09	0.080	--	--	--
2						0.049	--	--	--
3						0.020	0.29	0.14	0.90
4						0.014	--	--	--
5						0.007	0.50	0.50	0.50
6	5.06	2.00	0.40			0.008	0.25	0.50	0.38
7						0.030	0.43	0.21	0.77
8						0.040	0.32	0.21	0.86
9						0.063	--	--	0.81
10						0.089	--	--	--
11	9.84	1.03	0.20			0.014	0.14	0.71	0.48
12						0.030	0.20	0.63	0.46
13						0.040	0.15	0.52	0.71
14						0.070	0.19	0.70	0.80
15						0.080	0.16	0.39	0.82
16	14.50	0.70	0.14			0.010	0.12	0.82	0.32
17						0.030	0.14	0.55	0.68
18						0.050	0.45	0.37	0.66
19						0.059	0.26	0.36	0.80
20	18.70	0.54	0.107			0.011	0.33	1.00	0.11
21						0.041	0.29	0.40	0.76
22						0.040	0.45	0.53	0.52
23	4.53	1.20	0.22	0.50	0.22	0.022	0.20	0.60	0.60
24						0.040	0.11	0.50	0.74
25						0.060	0.11	0.44	0.80
26						0.077	0.20	0.40	0.80
27	7.72	0.70	0.13			0.012	0.11	0.89	0.20
28						0.018	0.29	0.93	0.05
29						0.030	0.13	0.74	0.43
30						0.039	0.13	0.63	0.38
31	10.76	0.51	0.09			0.009	0.30	1.00	0.09
32						0.020	0.19	0.86	0.22
33						0.030	0.16	0.75	0.41
34						0.038	0.20	0.68	0.50
35	5.06	1.08	0.39	0.25	0.11	0.030	--	--	--
36						0.050	--	--	--
37						0.073	--	--	--
38						0.081	--	--	--
39	9.84	0.54	0.20			0.021	0.24	0.95	0.04
40						0.032	0.16	0.84	0.26
41						0.046	0.18	0.64	0.56
42						0.052	0.14	0.67	0.53
43						0.048	0.19	0.83	0.27
44						0.074	0.16	0.73	0.44
45						0.082	--	--	--
46	14.50	0.38	0.14			0.018	0.15	0.85	0.26
47						0.023	0.06	0.79	0.38
48						0.029	0.07	0.79	0.38
49						0.037	0.06	0.74	0.45
50						0.041	0.08	0.77	0.40
51						0.047	0.19	0.78	0.35
52						0.054	0.11	0.73	0.46
53	4.53	0.51	0.22	0.50	0.22	0.022	--	--	--
54						0.042	0.26	0.53	0.65
55						0.064	0.24	0.72	0.42
56						0.067	0.23	0.77	0.73
57	7.72	0.30	0.13			0.013	0.09	1.00	0.00
58						0.026	0.10	0.90	0.18
59						0.035	0.07	0.93	0.12
60						0.042	--	--	--
61	10.76	0.22	0.09			0.009	0.10	1.00	0.01
62						0.016	0.18	0.88	0.20
63						0.022	0.17	0.63	0.57
64						0.030	0.19	0.88	0.19
65	5.06	0.46	0.39	0.25	0.11	0.030	--	--	--
66						0.053	--	--	--
67						0.076	--	--	--
68						0.087	--	--	--
69	9.84	0.24	0.20			0.025	0.13	0.96	0.06
70						0.030	0.07	0.97	0.05
71						0.040	0.13	0.92	0.13
72						0.048	0.11	0.91	0.16
73						0.051	0.14	0.94	0.10
74						0.069	0.13	0.91	0.15
					Tire Assembly (Continued)				
75	14.50	0.16	0.14	0.25	0.11	0.018	0.15	1.00	0.00
76						0.023	0.12	0.91	0.00
77						0.030	0.18	0.95	0.00
78						0.039	0.11	0.93	0.00
79						0.044	0.11	0.97	0.00
80						0.051	0.07	0.97	0.00
81						0.056	0.11	0.91	0.00
82	2.88	3.53	0.69	0.49	0.16	--	--	--	--
83						0.007	0.50	0.50	0.50
84						--	--	--	--
85						0.038	0.45	0.09	0.79
86						--	--	--	--
87	9.84	1.03	0.20			0.013	0.23	0.69	0.47
88						0.022	0.23	0.72	0.43
89						0.042	0.27	0.51	0.19
90						0.063	0.19	0.42	0.78
91						0.072	0.15	0.39	0.83
92	18.70	0.54	0.107			0.014	0.27	0.85	0.21
93						0.039	0.23	0.52	0.68
94						0.044	0.26	0.51	0.67
95	9.84	1.03	0.204	0.25	0.11	0.011	0.27	1.18	0.46
96						0.027	0.19	0.78	0.36
97						0.043	0.14	0.67	0.53
98						0.069	0.10	0.51	0.73
99						0.074	0.12	0.48	0.76
					Sphere Assembly				
1	4.53	0.56	0.22	0.60	0.26	0.020	0.22	0.22	0.90
2						0.049	0.14	0.27	0.91
3						0.060	0.33	0.37	0.75
4						0.053	0.42	0.42	0.64
5	7.72	0.33	0.13			0.018	--	0.64	--
6						0.027	0.24	0.76	0.36
7						0.040	0.23	0.71	0.45
8						0.051	0.23	0.85	0.23
9	10.76	0.24	0.09			0.010	0.18	0.91	0.14
10						0.016	0.12	0.94	0.11
11						0.023	0.20	0.88	0.19
12						0.032	0.24	0.91	0.11
13	5.06	0.50	0.39	0.30	0.13	0.018	0.33	0.33	0.78
14						0.053	--	--	--
15						0.075	--	--	--
16						0.087	--	--	--
17	9.84	0.26	0.20			0.025	0.08	0.84	0.28
18						0.032	0.25	0.78	0.33
19						0.035	0.12	0.91	0.16
20						0.050	0.04	0.75	0.44
21						0.062	--	--	--
22						0.084	--	--	--
23						--	--	--	--
24	14.50	0.18	0.14			0.017	0.12	1.04	0.09
25						0.023	0.21	0.91	0.13
26						0.030	0.27	0.98	0.03
27						0.036	0.27	1.02	0.80
28						0.043	0.13	1.00	0.02
29						0.049	0.11	1.03	0.07
30						0.059	0.12	0.90	0.18
31	4.53	1.33	0.22	0.60	0.26	0.020	0.22	0.22	0.90
32						0.042	0.16	0.37	0.83
33						0.053	0.17	0.37	0.83
34						0.064	0.38	0.38	0.72
35	7.72	0.78	0.13			0.014	0.27	0.64	0.52
36						0.021	0.38	0.69	0.38
37						0.040	0.23	0.52	0.68
38						0.040	0.15	0.61	0.61
39	10.76	0.56	0.09			0.012	0.31	0.85	0.18
40						0.022	0.04	0.79	0.38
41						0.031	0.18	0.76	0.39
42						0.039	0.38	0.76	0.28
43	5.06	1.18	0.39	0.30	0.13	0.032	--	--	0.86
44						0.055	--	--	0.83
45						0.077	--	--	--
46						0.083	--	--	--

(Continued)

Sphere Assembly (Continued)

No.	L, ft	w/L	d/L	y/d	h/d	H_i/L	K_r	K_t	P_D/P
56	9.84	0.61	0.39	0.30	0.13	0.028	0.18	0.64	0.56
57						0.031	0.30	0.70	0.42
58						0.037	0.25	0.72	0.42
59						0.046	0.29	0.67	0.47
60						0.056	0.31	0.60	0.54
61						0.082	--	--	--
62						0.087	--	--	--
63	14.50	0.41	0.14			0.015	0.14	0.86	0.24
64						0.021	0.13	0.77	0.39
65						0.027	0.10	0.69	0.51
66						0.034	0.10	0.66	0.55
67						0.040	0.21	0.69	0.48
68						0.045	0.15	0.44	0.79
69						--	--	--	--
70	2.88	3.47	0.69			0.010	0.33	0.33	0.78
71						0.013	--	--	--
72						0.024	0.14	0.14	0.96
73						0.049	--	--	--
74						0.080	--	--	--

Sphere Assembly (Continued)

No.	L, ft	w/L	d/L	y/d	h/d	H_i/L	K_r	K_t	P_D/P
66	5.06	1.98	0.40	0.30	0.13	0.004	0.50	0.50	0.71
67						0.022	0.18	0.18	0.94
68						0.038	0.37	0.11	0.85
69						0.067	--	--	--
70						0.083	--	--	--
71	9.84	1.02	0.20			0.009	0.33	0.89	0.10
72						0.027	0.26	0.74	0.38
73						0.035	0.06	0.79	0.38
74						0.065	0.22	0.50	0.70
75						0.072	0.18	0.51	0.71
76	14.50	0.69	0.14			0.010	0.47	1.20	0.09
77						0.023	0.27	0.88	0.16
78						0.042	0.16	0.69	0.49
79						0.050	0.19	0.61	0.59
80	18.70	0.54	0.107			0.013	0.21	0.96	0.04
81						0.037	0.16	0.73	0.44
82						0.046	0.21	0.65	0.54

Table 4

$f_c/f_{t_{max}}$, Tire and Sphere Assemblies

Test No.	L, ft	$\frac{2\pi d}{L}$	$\tanh \frac{2\pi d}{L}$	$f_{t_{max}} \times 10^3$ ft of Water	(h + y) ft	$f_{c1} \times 10^3$ ft of Water	$f_{c2} \times 10^3$ ft of Water	w/L	$f_{c1}/f_{t_{max}}$	$f_{c2}/f_{t_{max}}$
				Tire Assembly						
1	2.88	4.36	1.00	--	1.30	--	--	3.52	--	--
2	↓	↓	↓	--	↓	--	--	↓	--	--
3				--		--	--		--	--
4				--		--	--		--	--
5				59.6		3.33	--		0.06	--
6	5.06	2.48	0.99	--		--	--	2.00	--	--
7	↓	↓	↓	60.5		3.33	2.00	↓	0.06	0.03
8				101		9.16	2.62		0.09	0.03
9				141		23.3	3.95		0.17	0.03
10				185		39.9	7.92		0.22	0.04
11	9.84	1.28	0.86	67.1		3.33	14.5	1.03	0.05	0.22
12	↓	↓	↓	201		37.1	24.1	↓	0.18	0.12
13				329		73.3	34.1		0.22	0.10
14				464		133	43.7		0.29	0.09
15				598		158	50.4		0.26	0.08
16	14.5	0.86	0.69	120		10.0	20.4	0.70	0.08	0.17
17	↓	↓	↓	353		58.4	46.3	↓	0.16	0.13
18				586		162	59.0		0.28	0.10
19				626		175	65.5		0.28	0.10
20	18.7	0.67	0.59	167		13.3	12.5	0.54	0.08	0.07
21	↓	↓	↓	493	↓	104	48.7	↓	0.21	0.10
22				590		129	53.3		0.22	0.09
				Sphere Assembly						
1	2.88	4.36	1.00	2.29	0.86	--	--	3.47	--	--
2	↓	↓	↓	--	↓	--	--	↓	--	--
3				--		--	--		--	--
4				32.1		3.06	--		0.01	--
5				52.8		15.3	2.04		0.29	0.04
6	5.06	2.48	0.99	--		--	--	1.97	--	--
7	↓	↓	↓	44.4		5.1	2.0	↓	0.11	0.45
8				76.5		15.3	3.0		0.20	0.04
9				137		40.8	6.0		0.30	0.04
10				169		56.2	10.0		0.33	0.06
11	9.84	1.28	0.86	60.5		5.11	9.8	1.12	0.08	0.16
12	↓	↓	↓	181		28.5	17.8	↓	0.16	0.10
13				228		76.8	31.4		0.34	0.14
14				430		194	66.8		0.45	0.16
15				477		224	70.7		0.47	0.15
16	14.5	0.86	0.69	120		15.3	18.7	0.69	0.13	0.16
17	↓	↓	↓	265		30.6	23.4	↓	0.12	0.09
18				489		76.8	51.6		0.16	0.11
19				578		153	70.4		0.26	0.12
20	18.7	0.67	0.59	185		10.2	24.0	0.54	0.06	0.13
21	↓	↓	↓	590		76.8	35.7	↓	0.13	0.06
22				660	↓	92.0	40.3		0.14	0.06

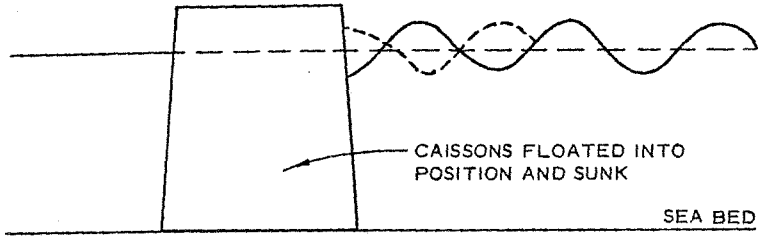

a. WAVE REFLECTION

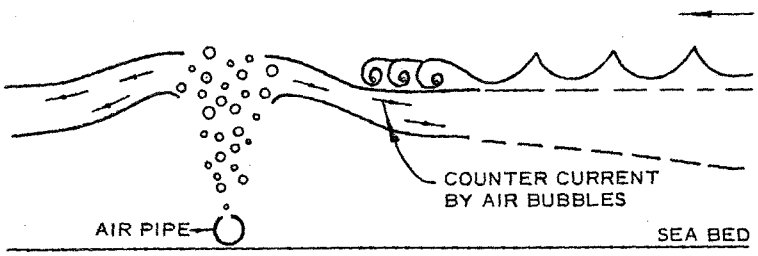

b. DISSIPATION OF WAVE ENERGY BY BREAKING

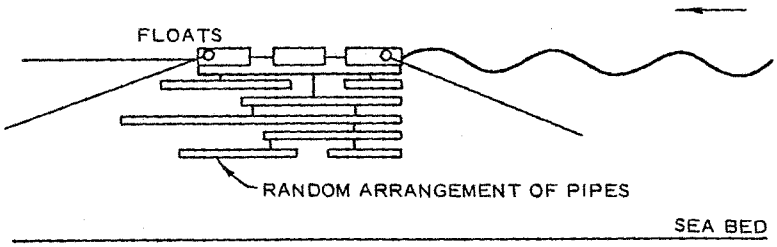

c. DESTRUCTION OF WAVE ORBITAL MOTION

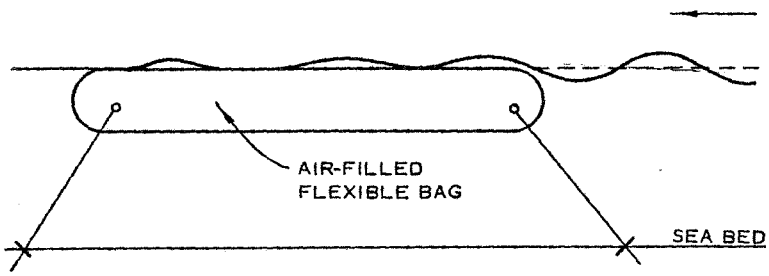

d. OUT-OF-PHASE DAMPING

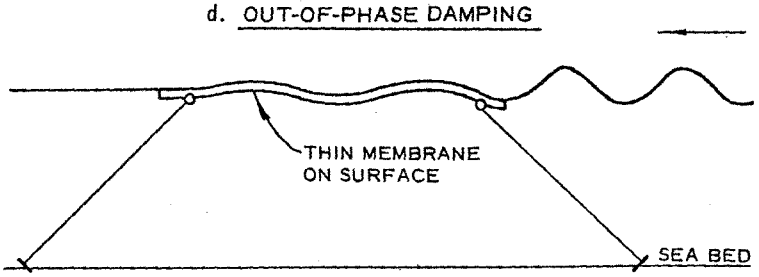

e. VISCOUS DAMPING

METHODS OF WAVE ATTENUATION

AFTER BULSON[11]

PLATE I

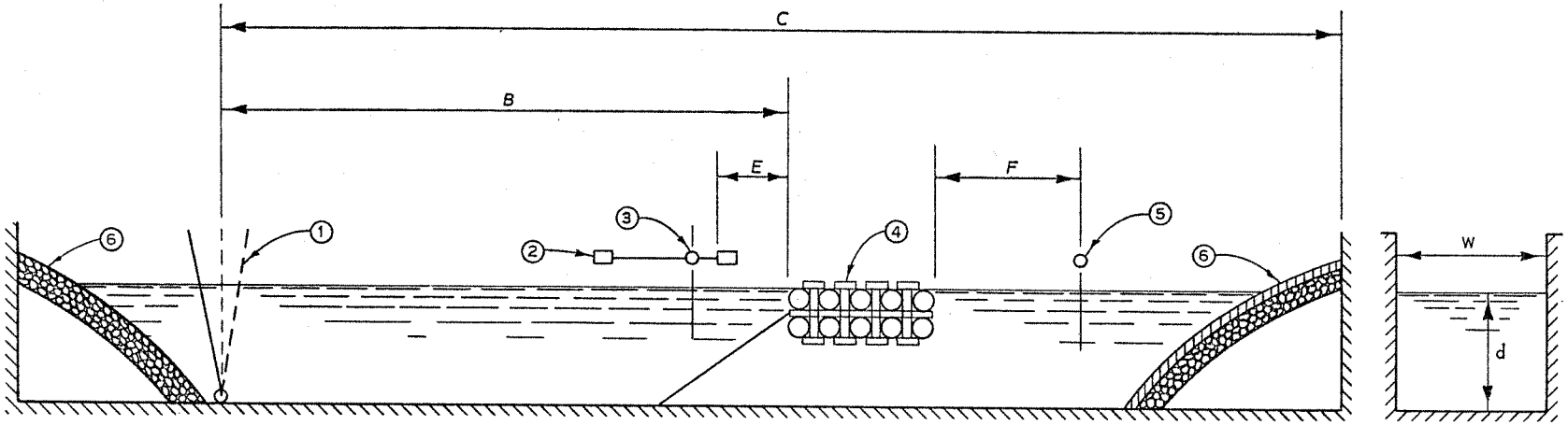

CHANNEL ELEVATION

CHANNEL SECTION

FIGURES		DIMENSIONS
①	WAVE GENERATOR	W = 2'
②	SAGINAW SCREW	d = 1, 2'
③	INCIDENT AND REFLECTED WAVE ROD	B = 100'
④	TEST STRUCTURE	C = 150'
⑤	TRANSMITTED WAVE ROD	E = 5.0'
⑥	PERMEABLE ABSORBER	F = 1 WAVE LENGTH

TYPICAL LAYOUT OF TEST FACILITIES

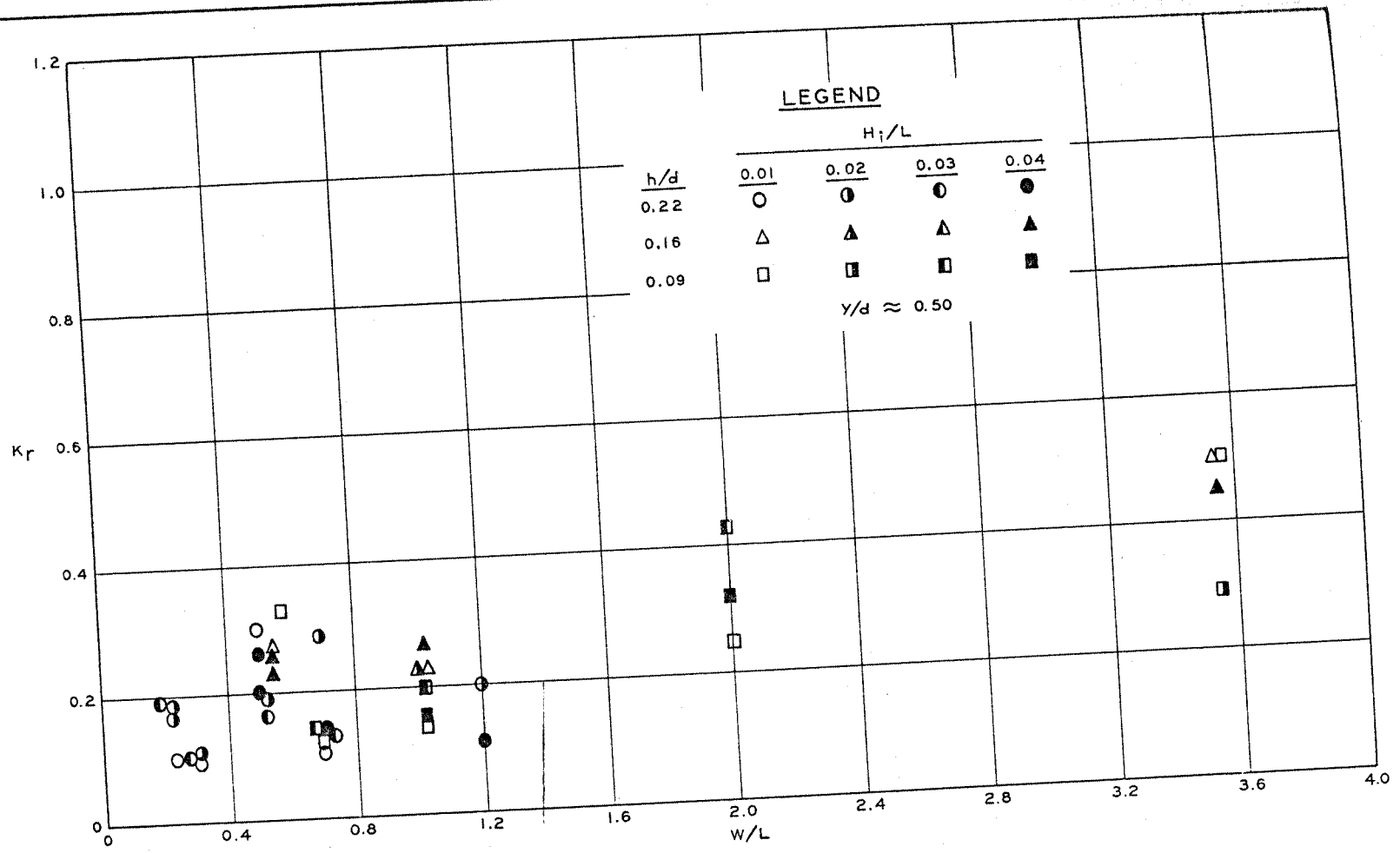

EFFECT OF h/d ON Kr

TIRE ASSEMBLY

PLATE 3

PLATE 4

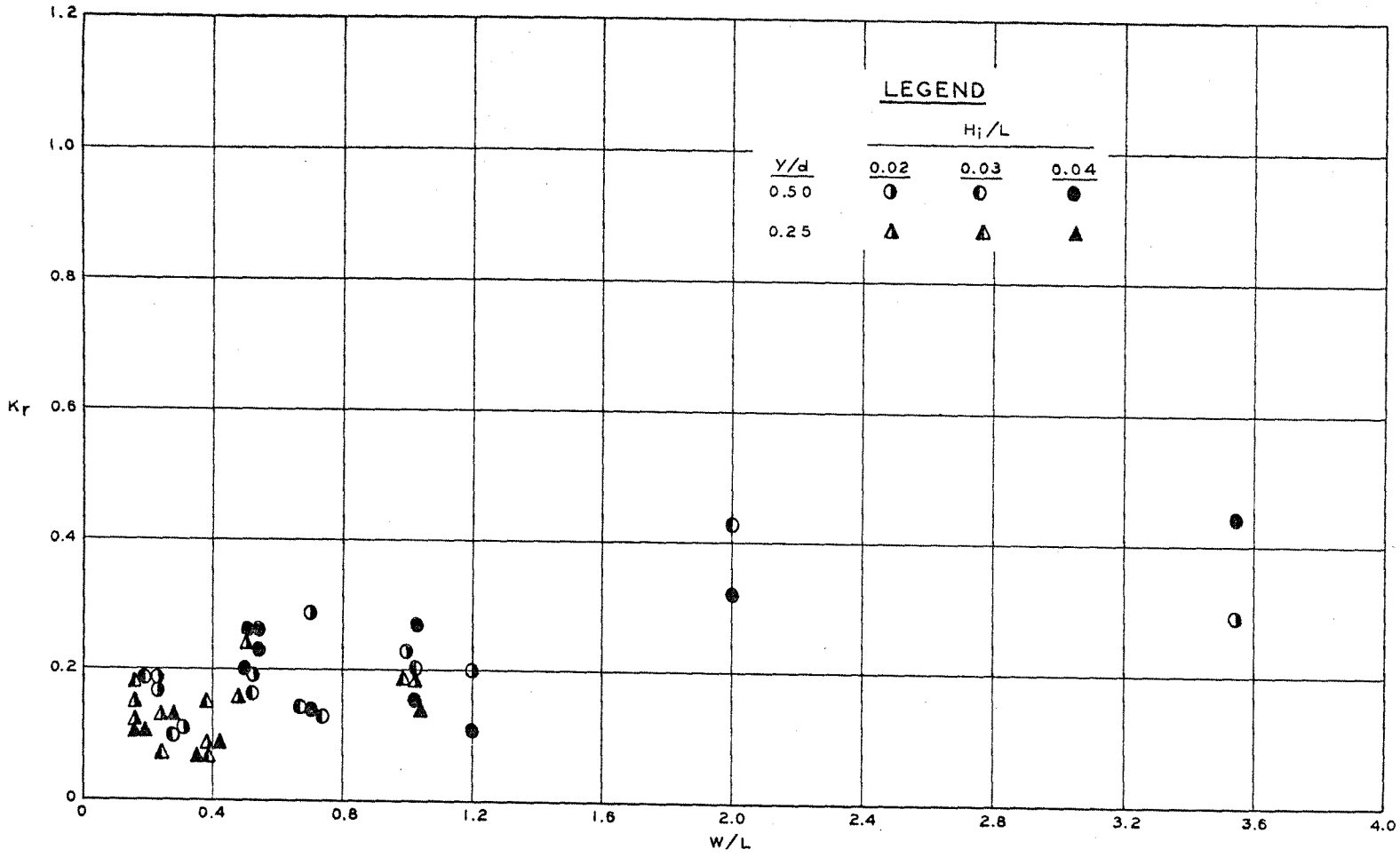

EFFECT OF y/d ON K_r

TIRE ASSEMBLY

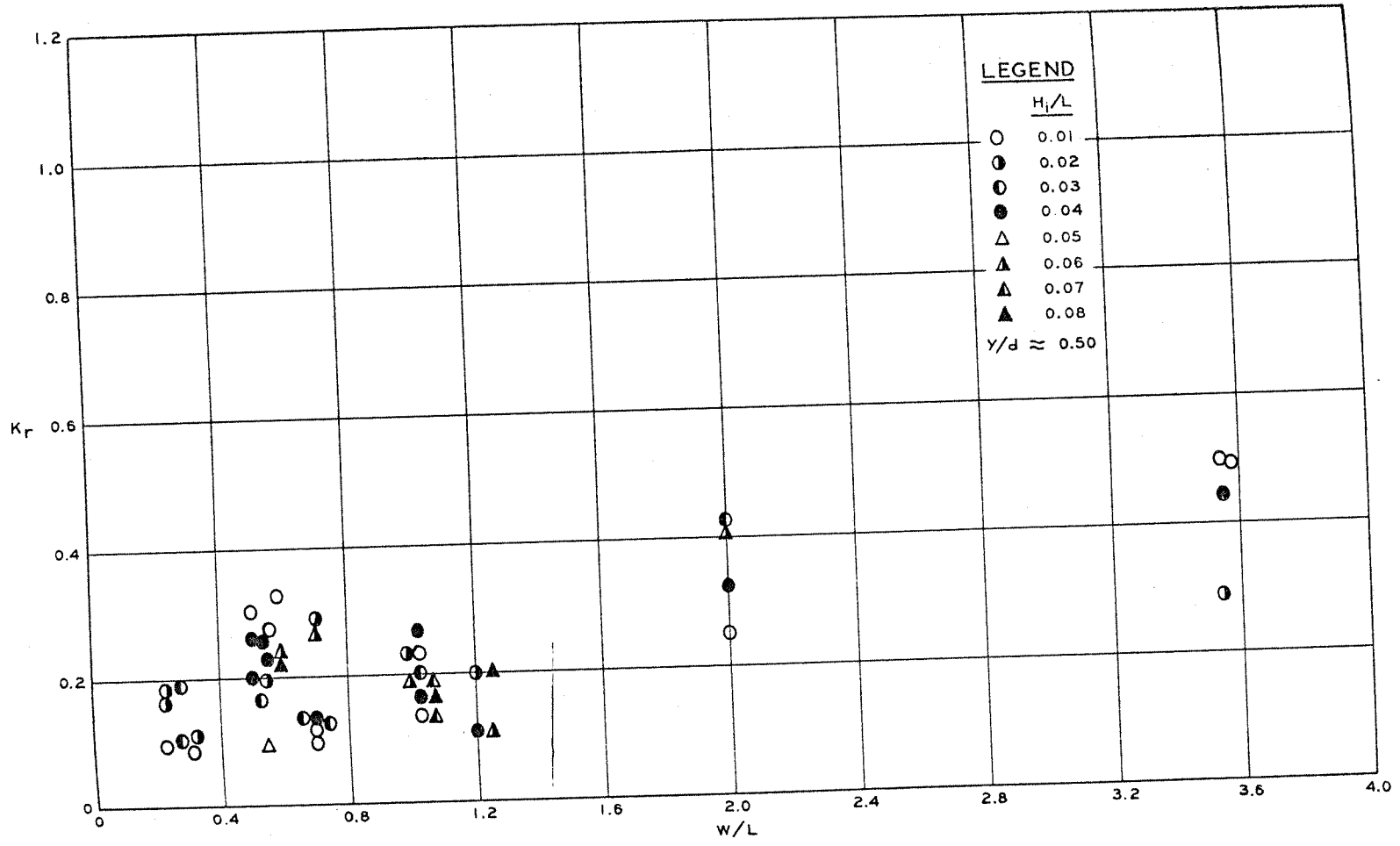

EFFECT OF H_i/L ON K_r

TIRE ASSEMBLY

PLATE 5

PLATE 6

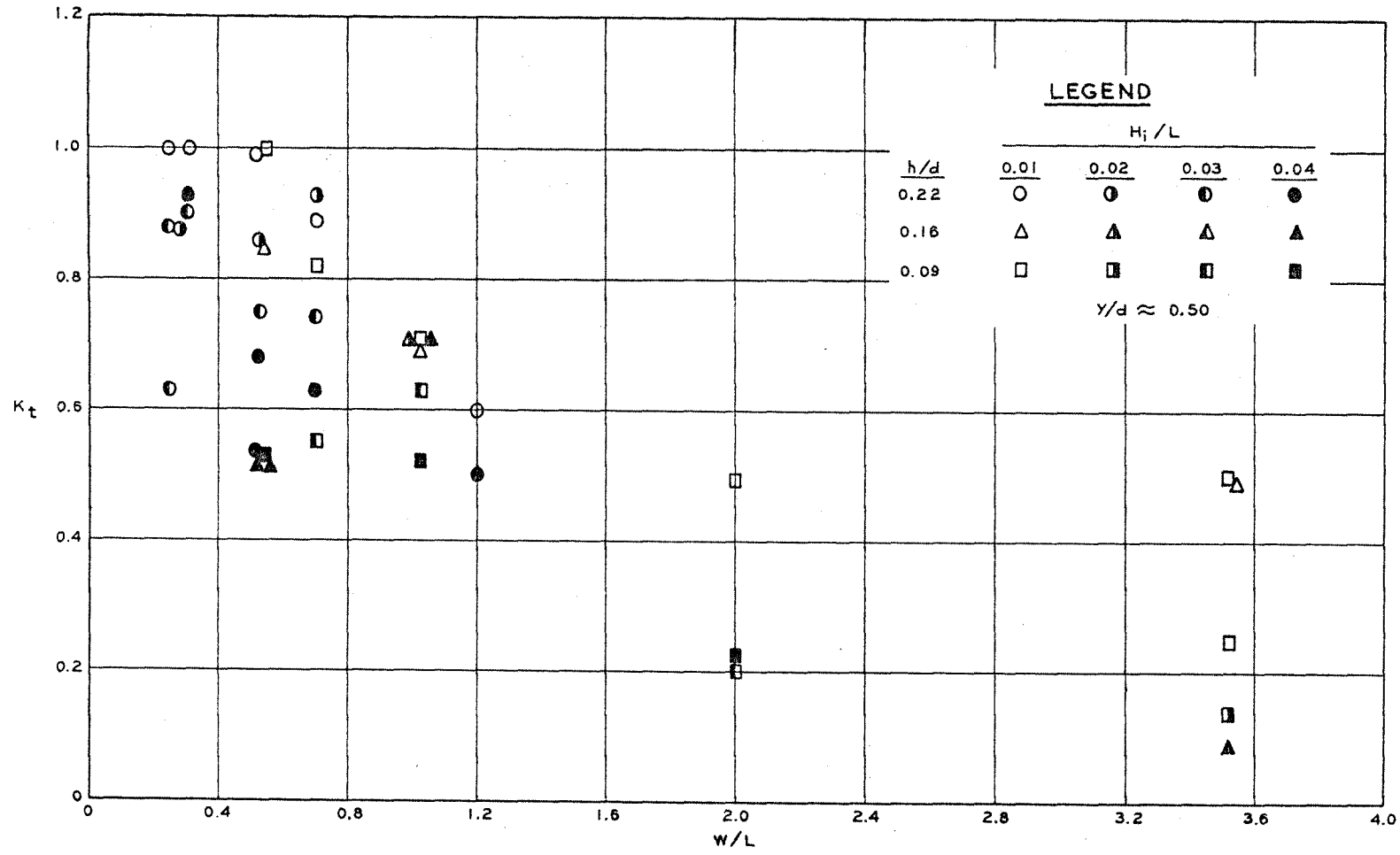

EFFECT OF h/d ON K_t

TIRE ASSEMBLY

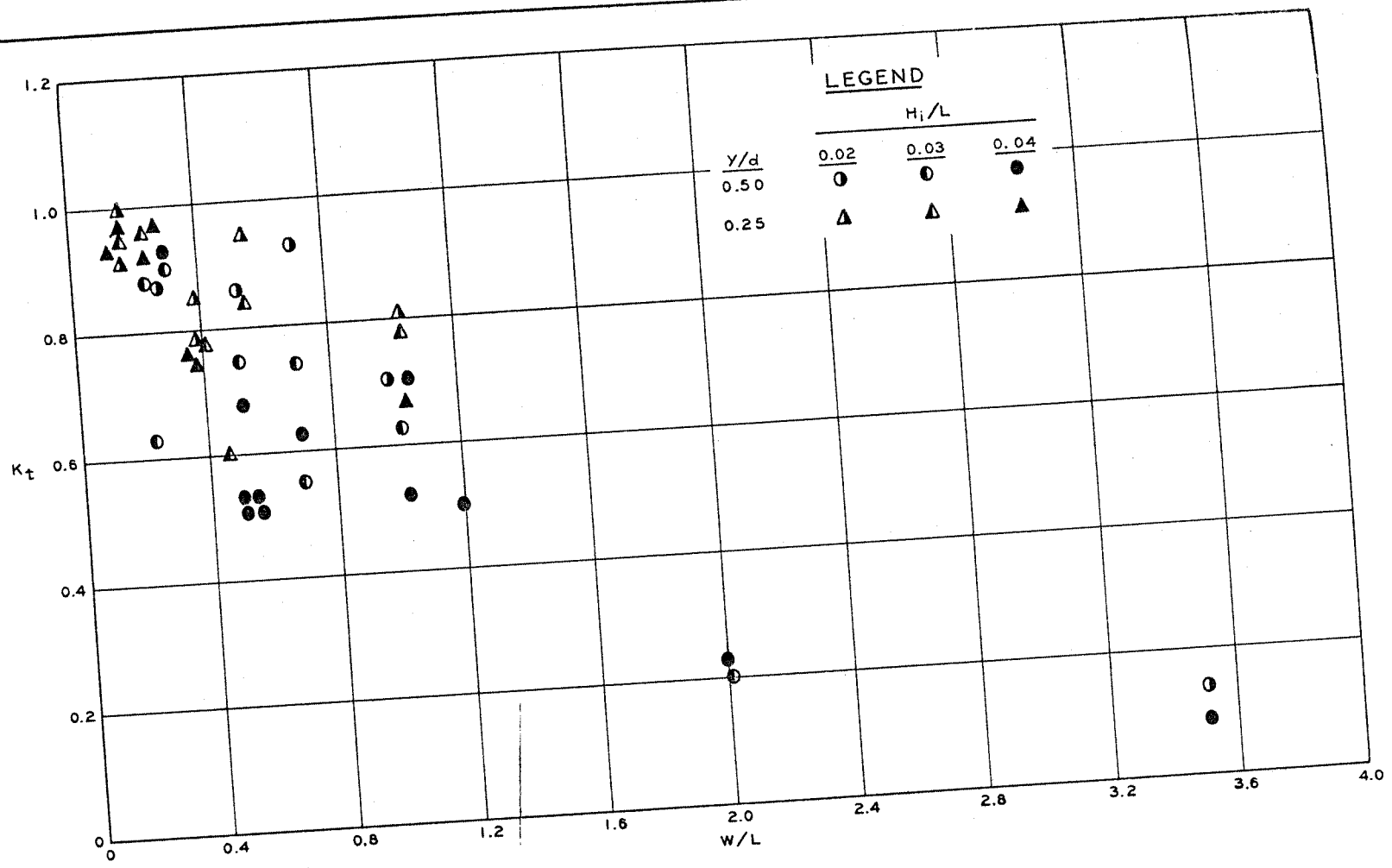

EFFECT OF y/d ON K_t

TIRE ASSEMBLY

PLATE 7

PLATE 8

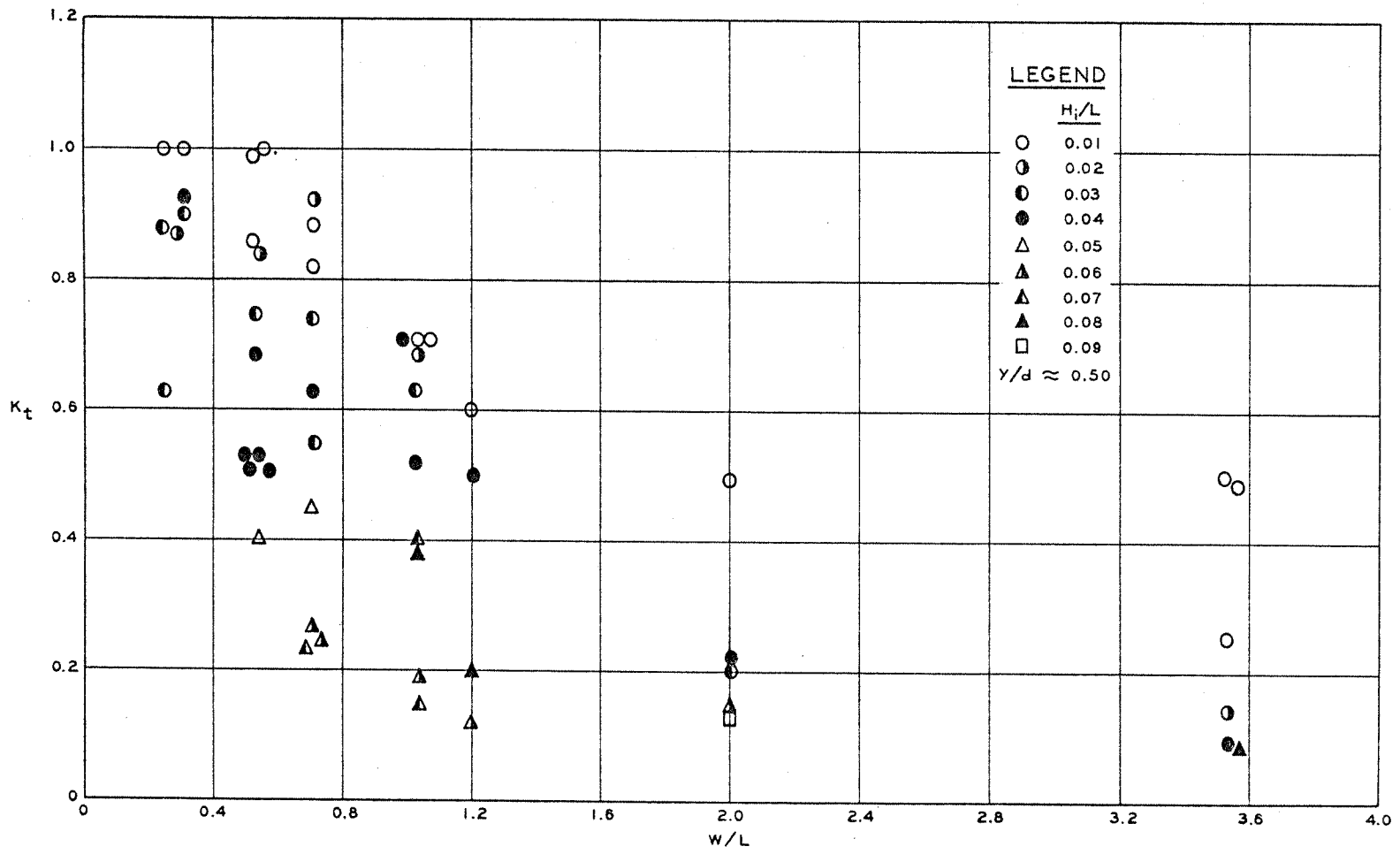

EFFECT OF H_i/L ON K_t

TIRE ASSEMBLY

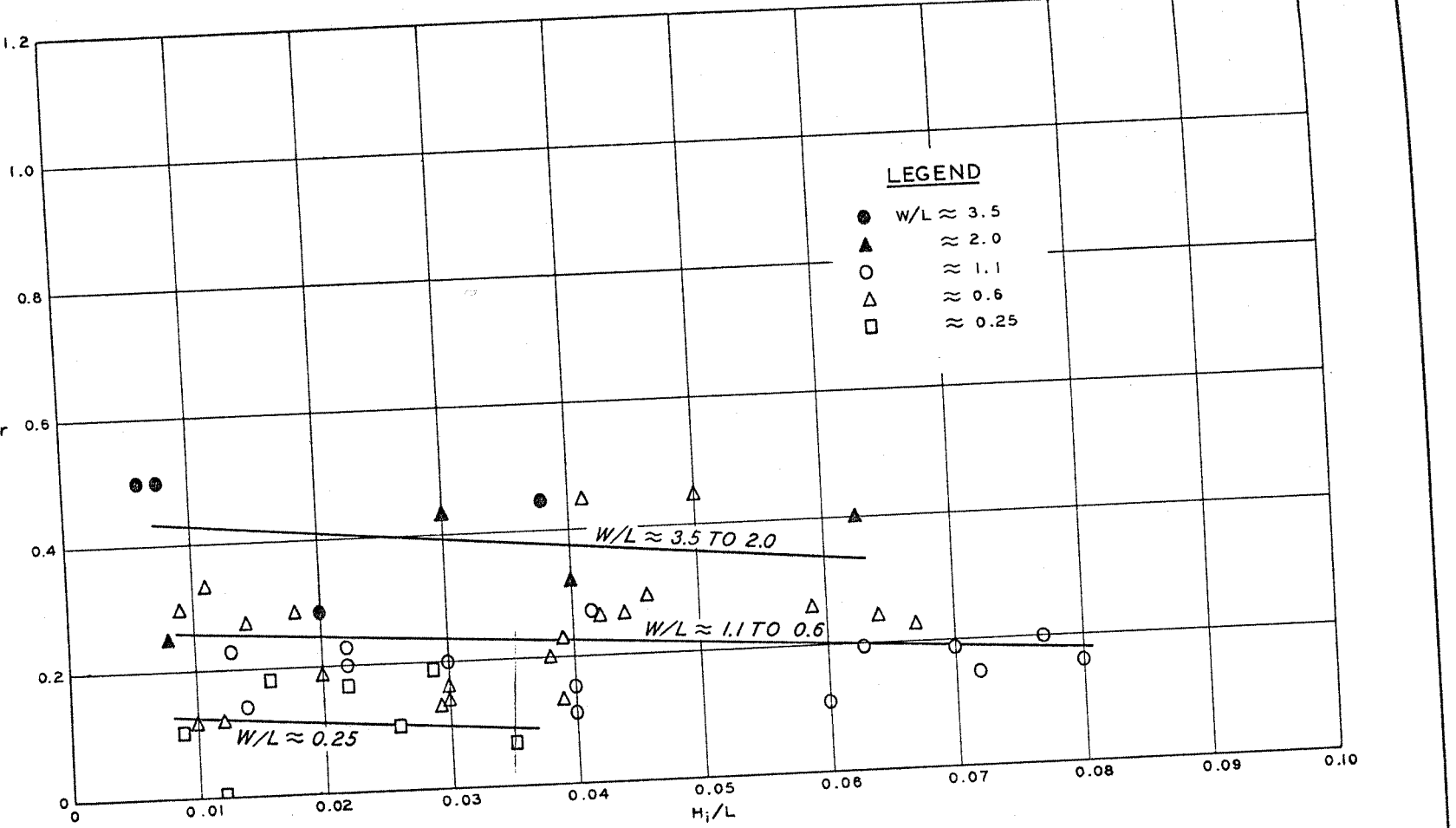

Kr VERSUS Hi/L

TIRE ASSEMBLY

y/d ≈ 0.50

PLATE 10

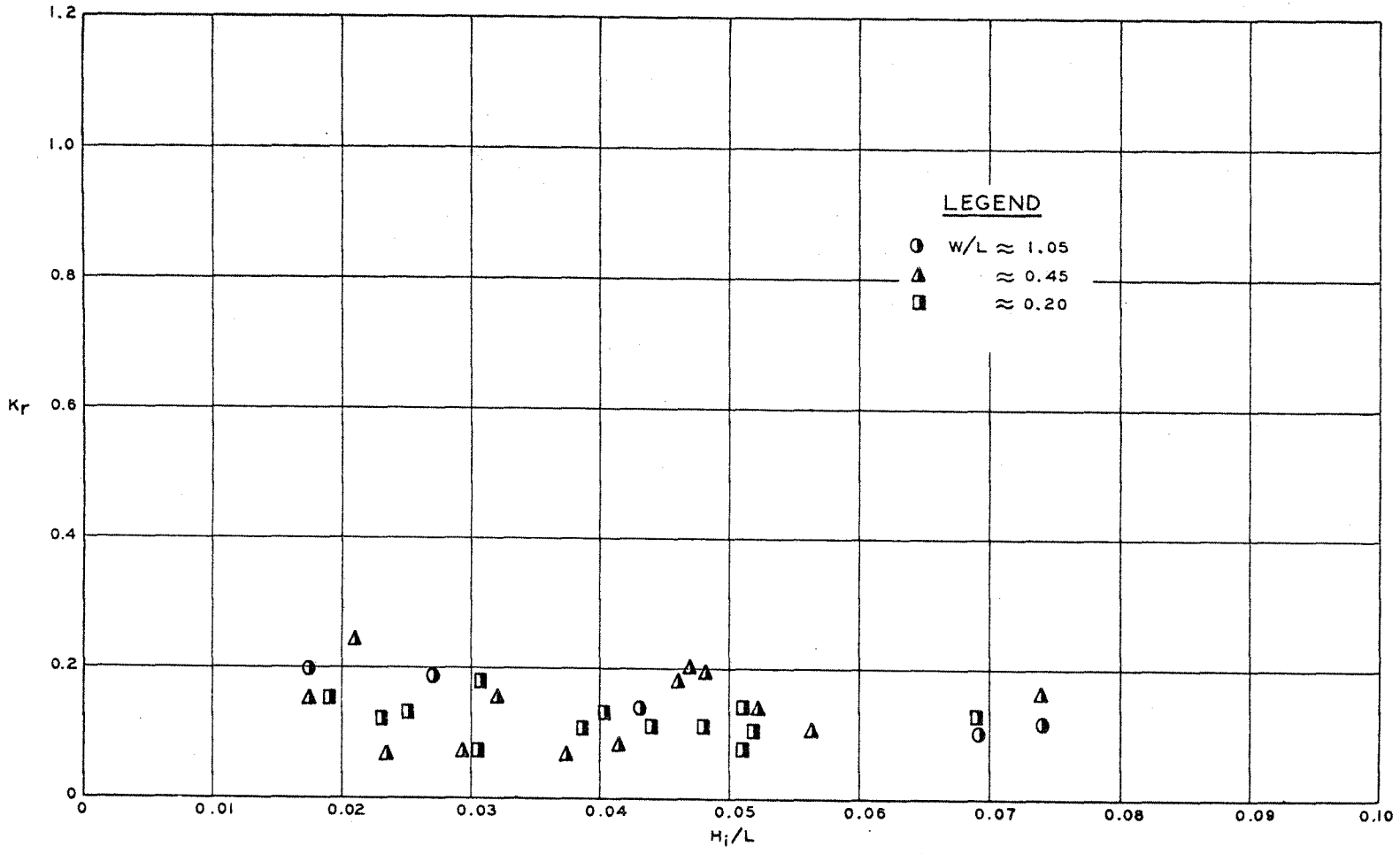

K_r VERSUS H_i/L

TIRE ASSEMBLY

$y/d = 0.25$

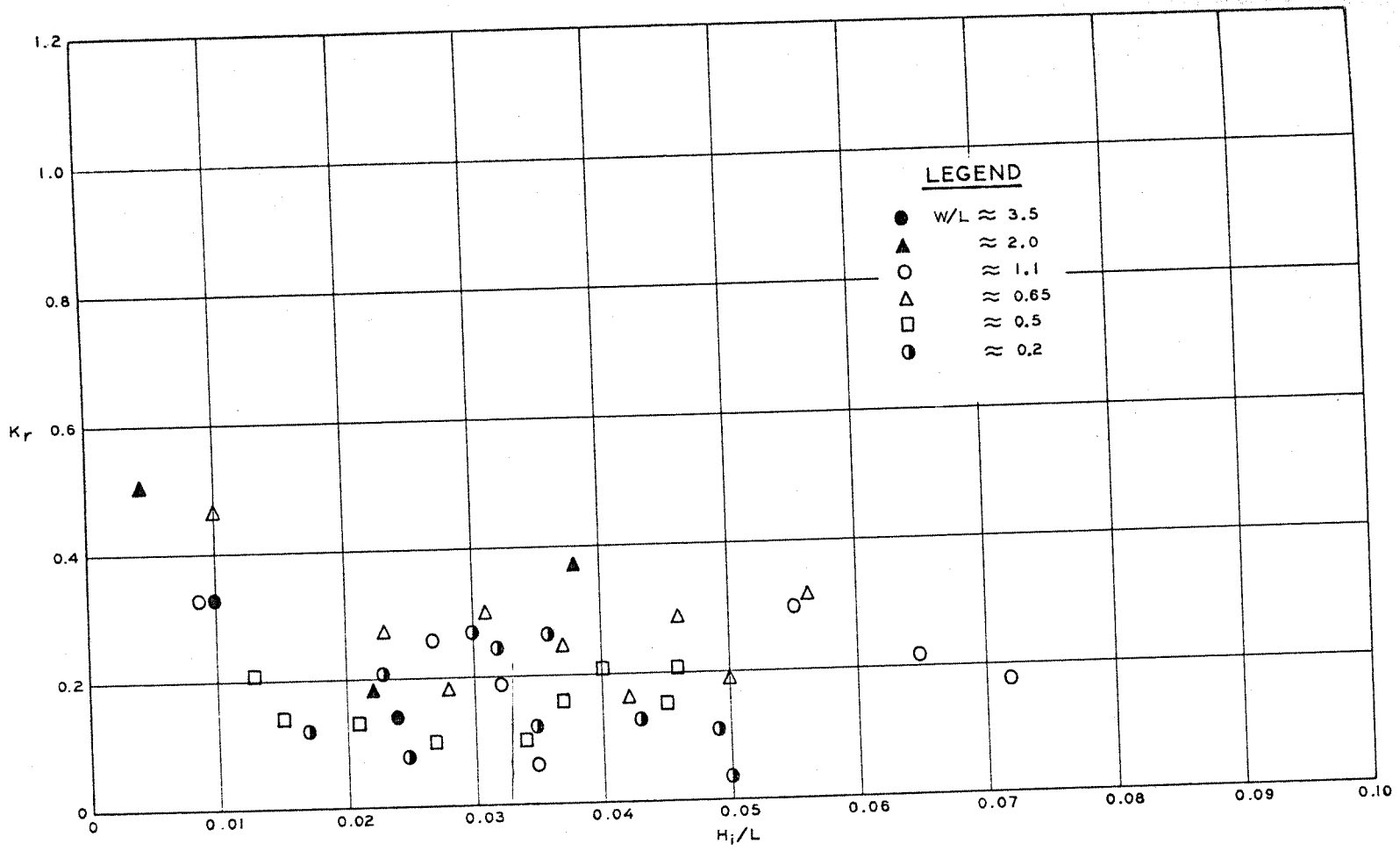

K_r VERSUS H_i/L

SPHERE ASSEMBLY

$y/d = 0.3$

PLATE 11

PLATE 12

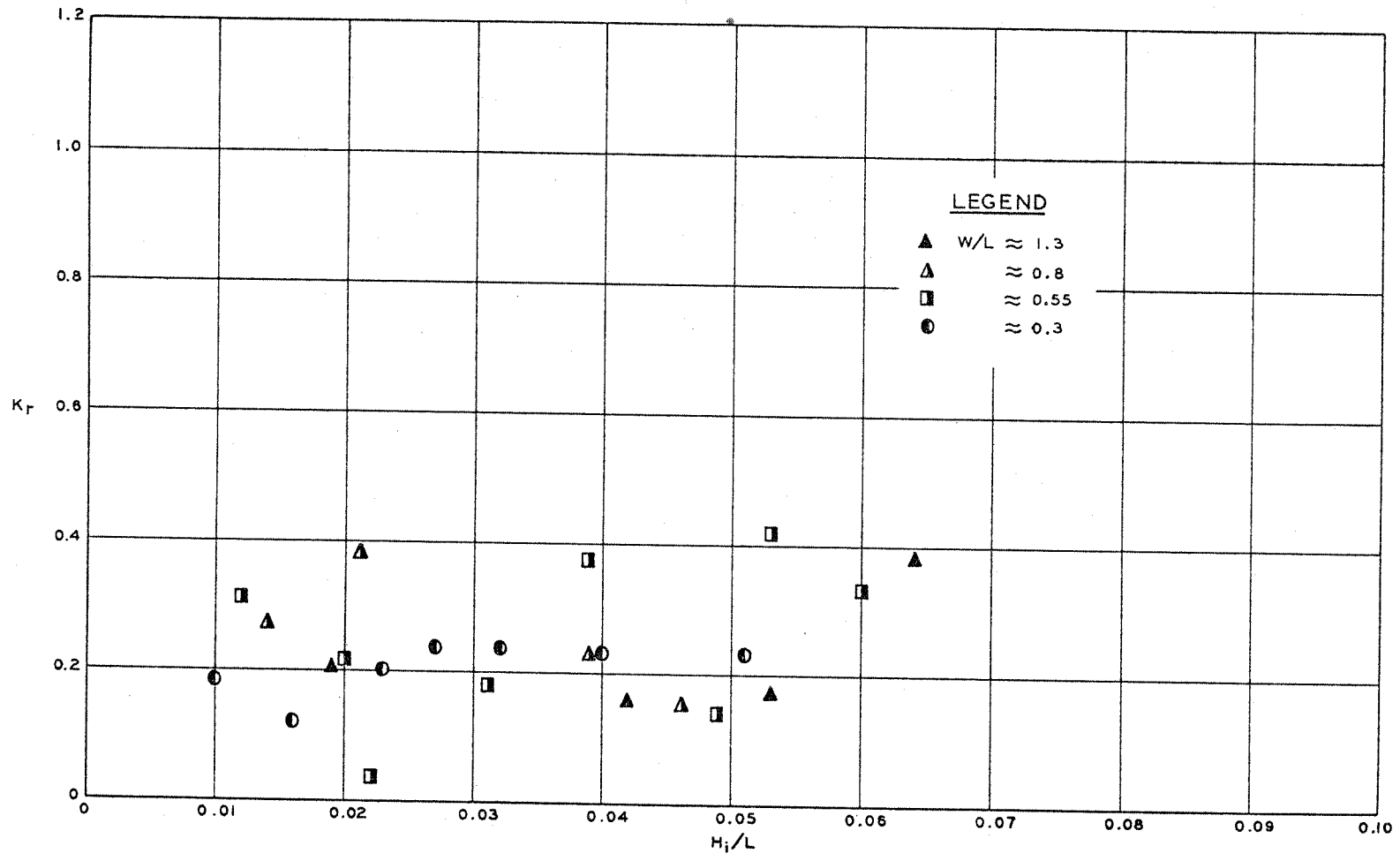

K_r VERSUS H_i/L

SPHERE ASSEMBLY

$y/d = 0.6$

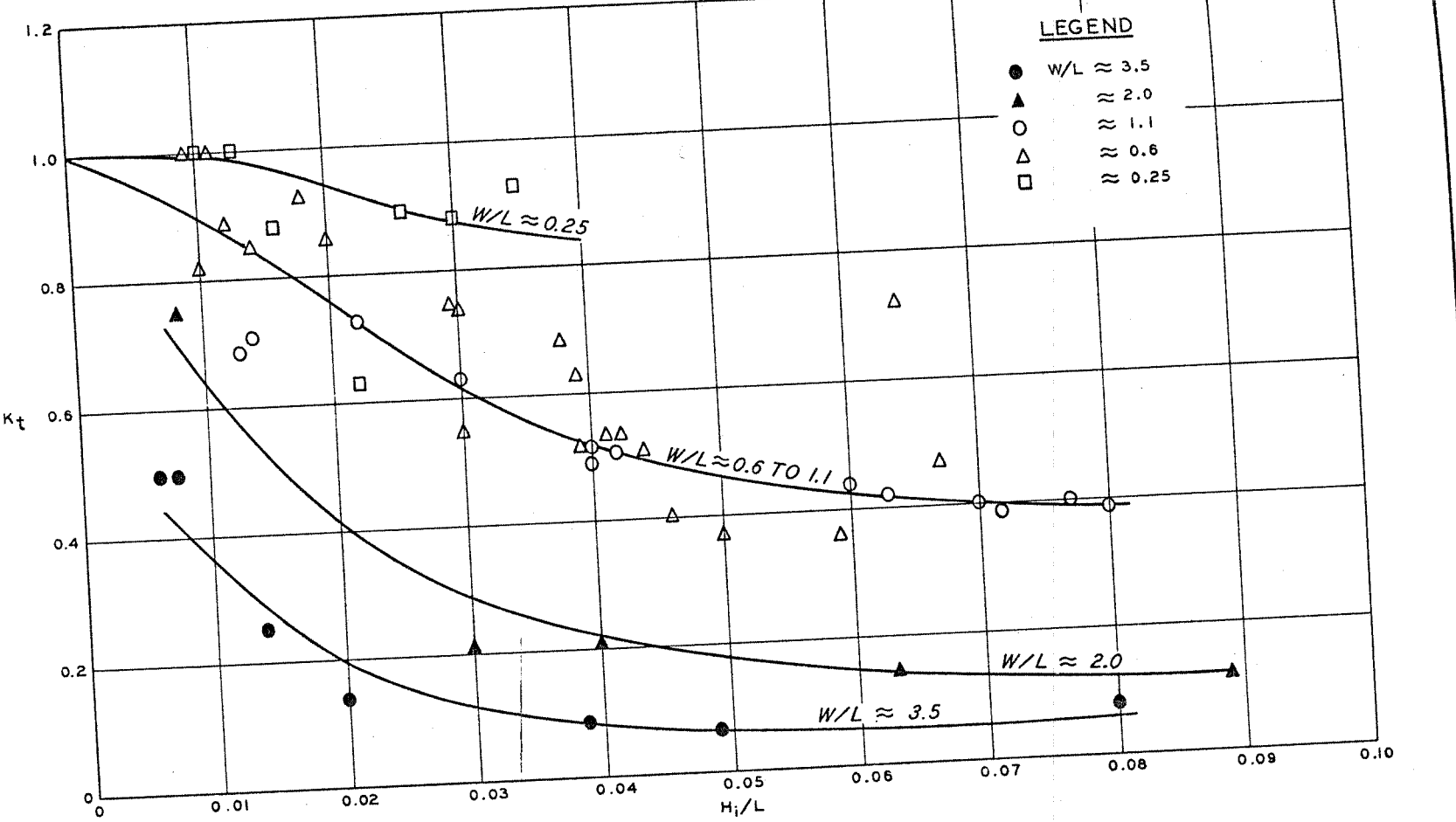

K_t VERSUS H_i/L

TIRE ASSEMBLY

$y/d \approx 0.50$

PLATE 14

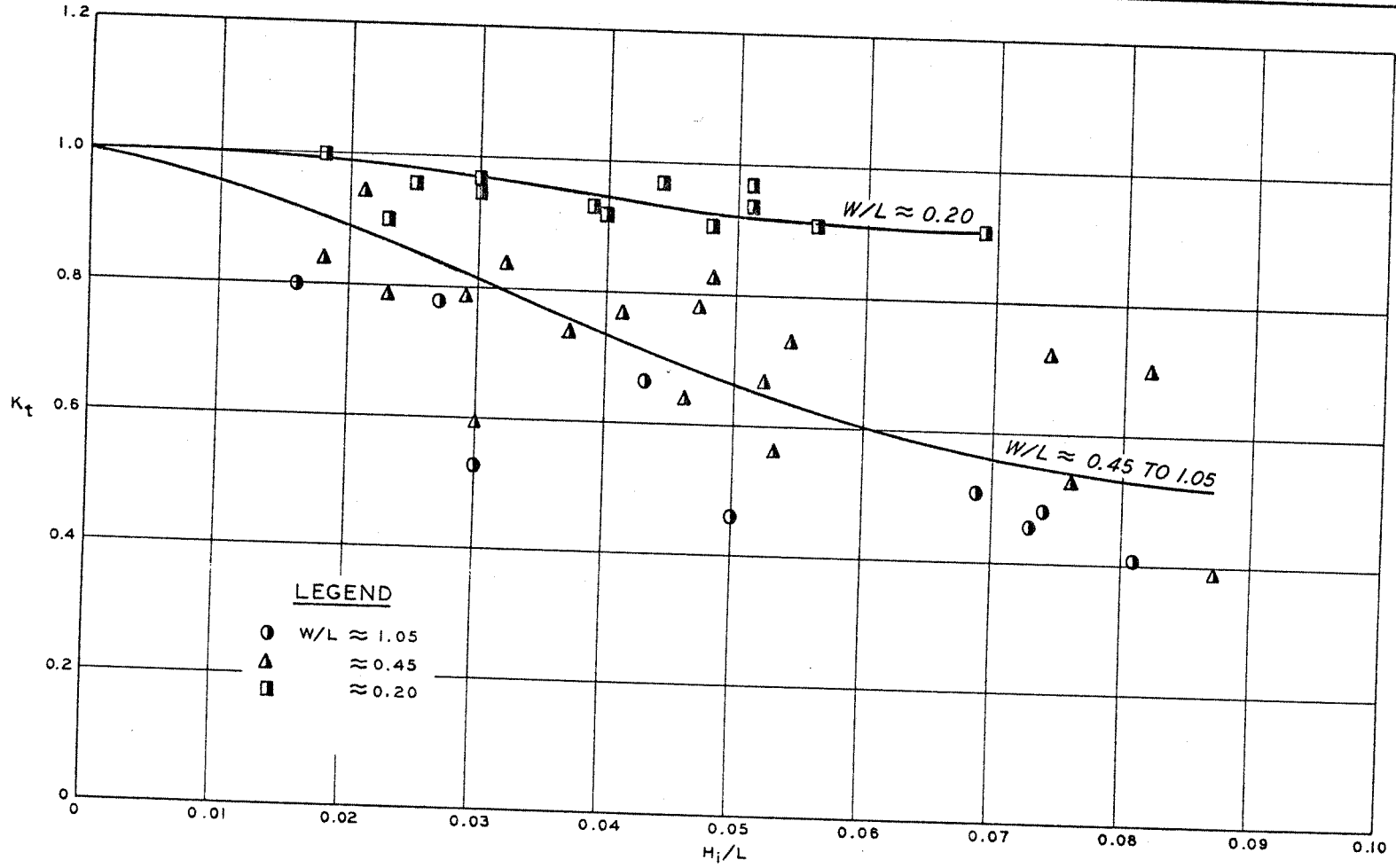

K_t VERSUS H_i/L

TIRE ASSEMBLY

$y/d = 0.25$

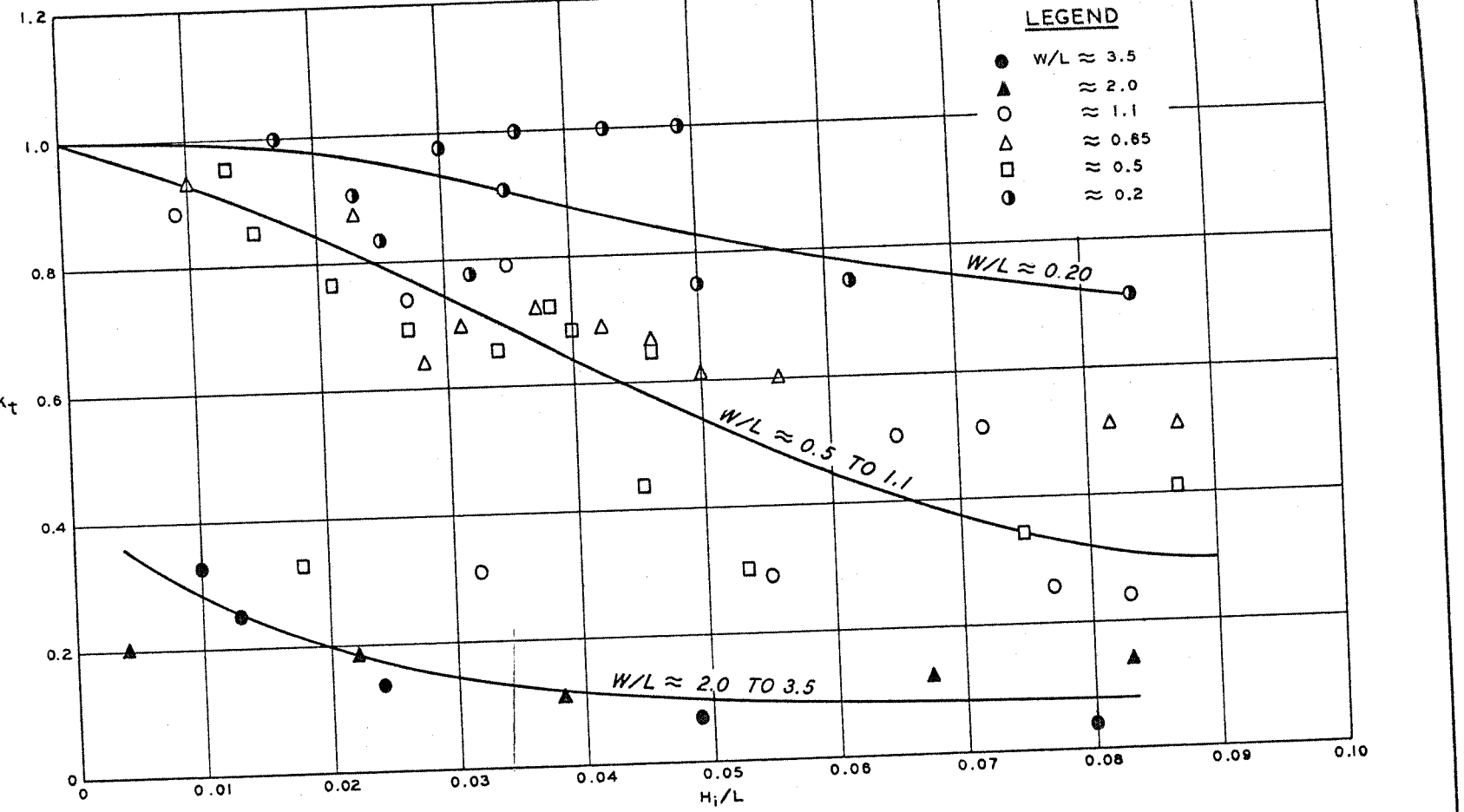

K_t VERSUS H_i/L

SPHERE ASSEMBLY

$y/d = 0.3$

PLATE 16

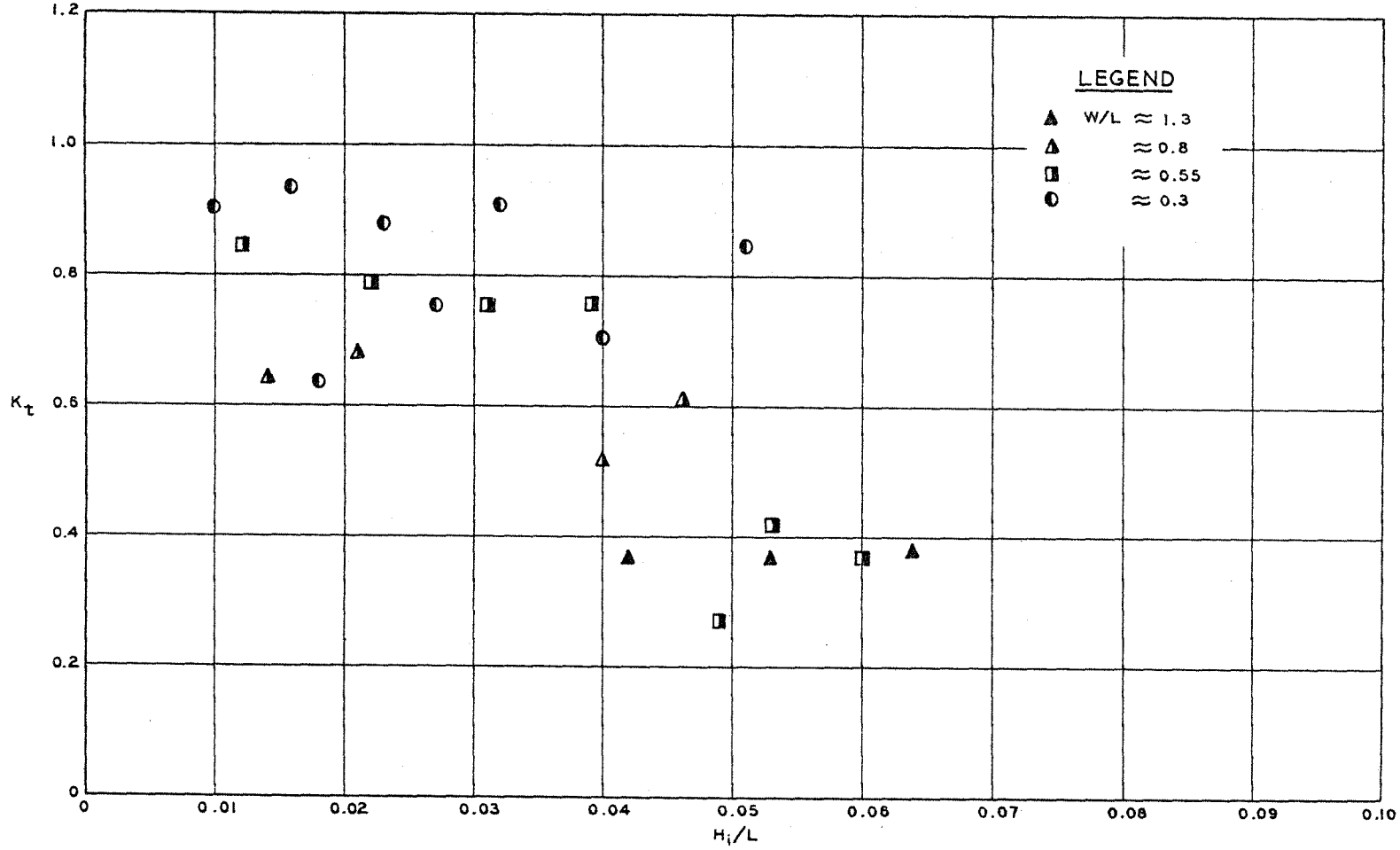

K_t VERSUS H_i/L

SPHERE ASSEMBLY

$y/d = 0.6$

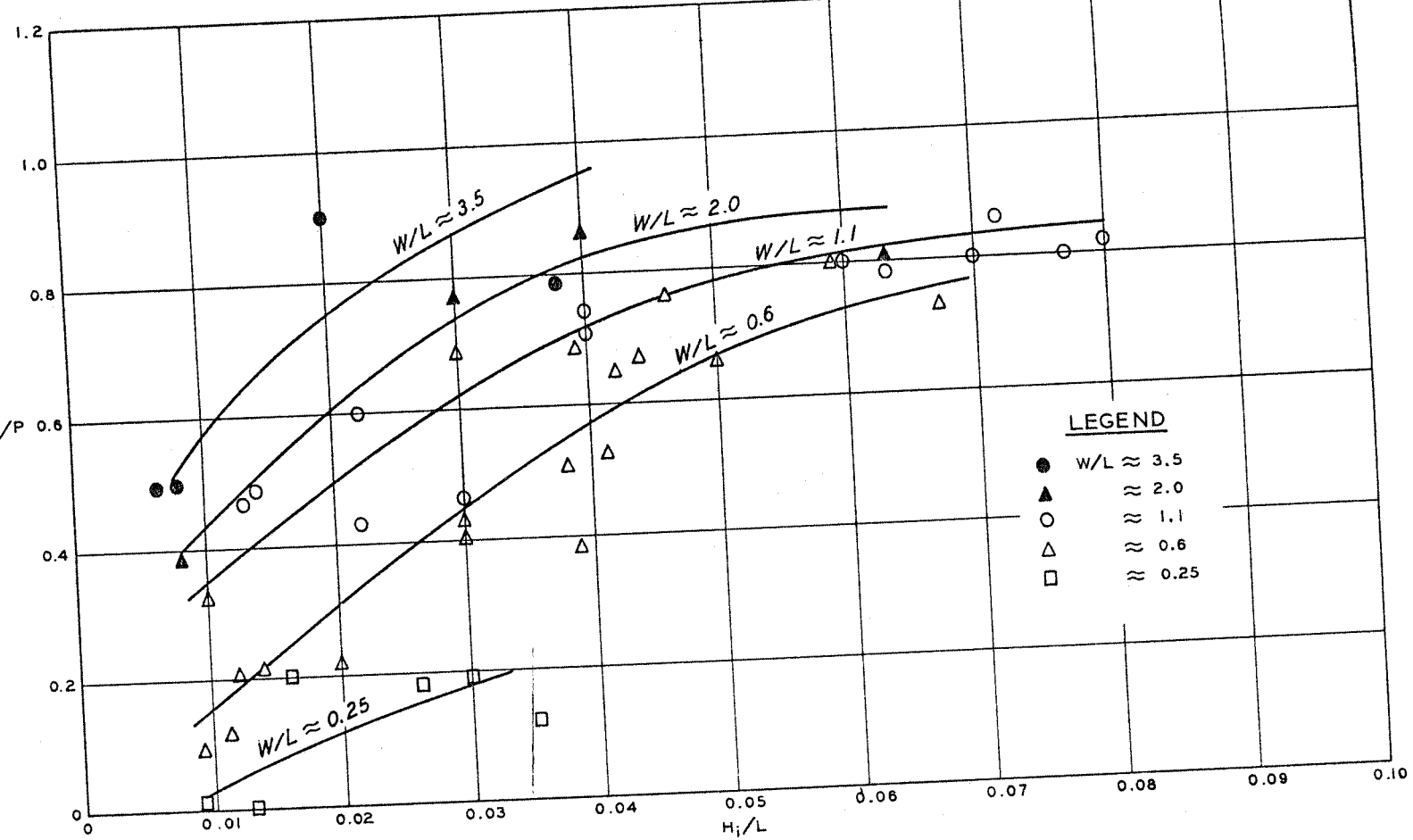

P_D/P VERSUS H_i/L

TIRE ASSEMBLY

$y/d \approx 0.50$

PLATE 18

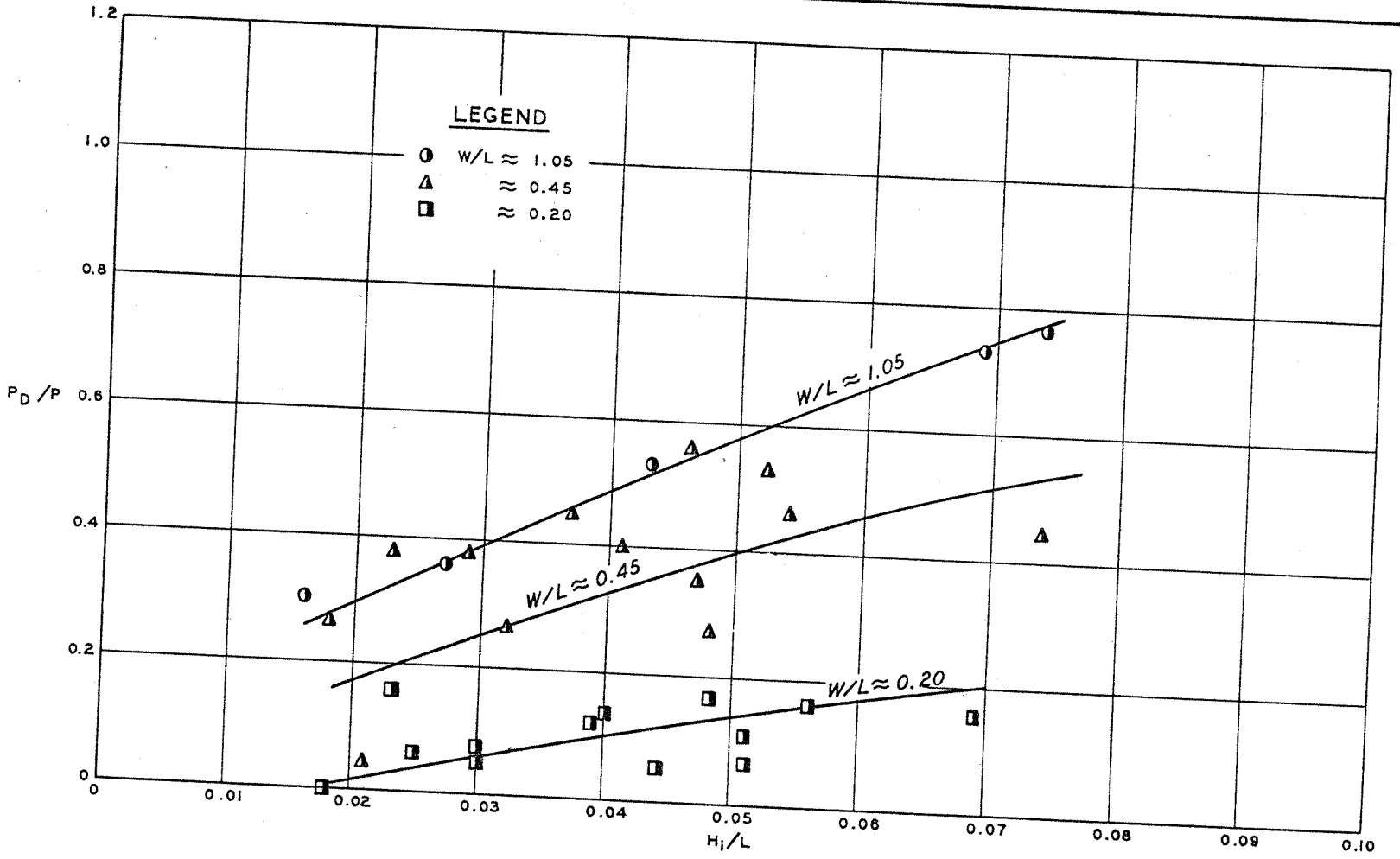

P_D/P VERSUS H_i/L

TIRE ASSEMBLY

$y/d = 0.25$

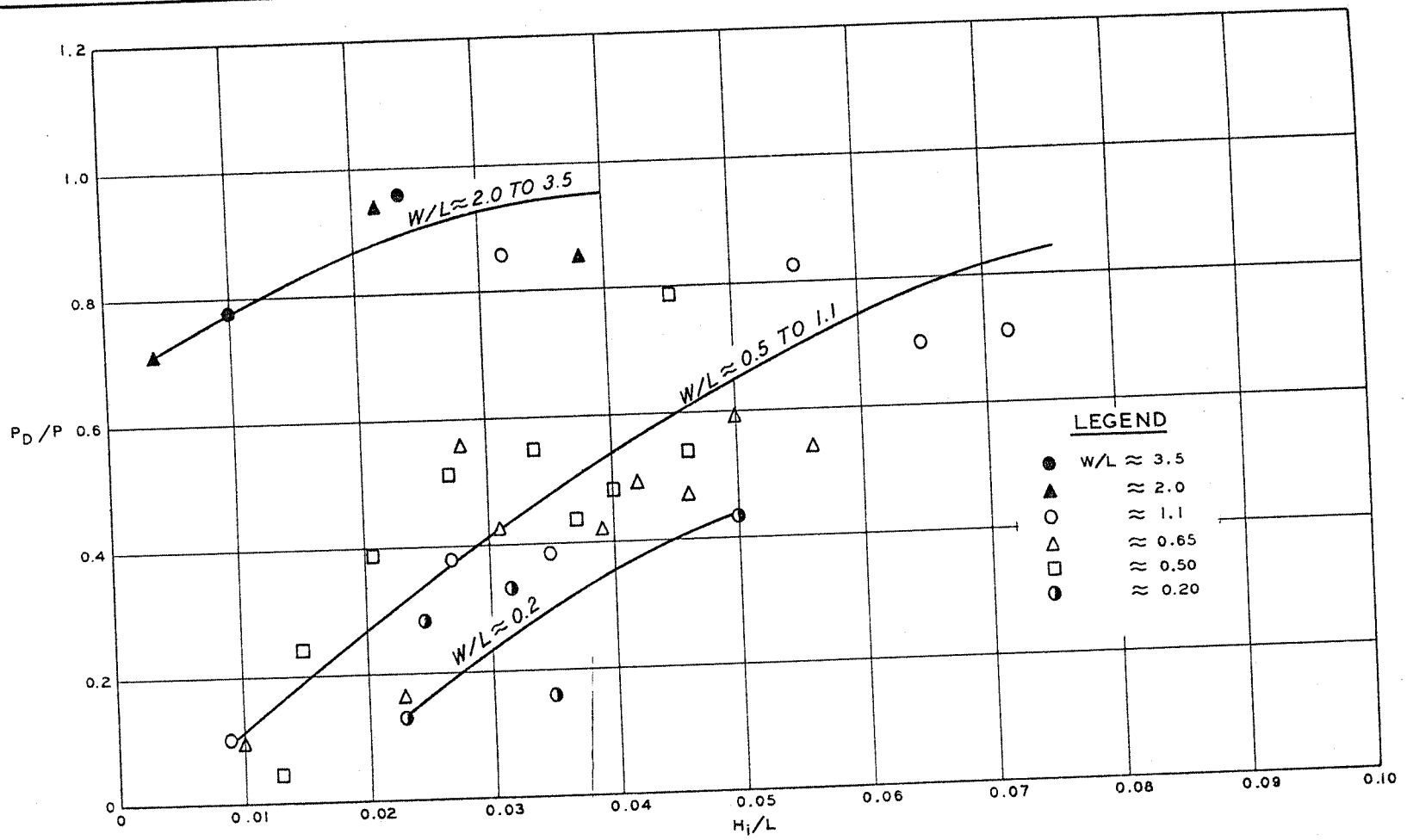

P_D/P VERSUS H_i/L

SPHERE ASSEMBLY

$y/d = 0.3$

PLATE 19

PLATE 20

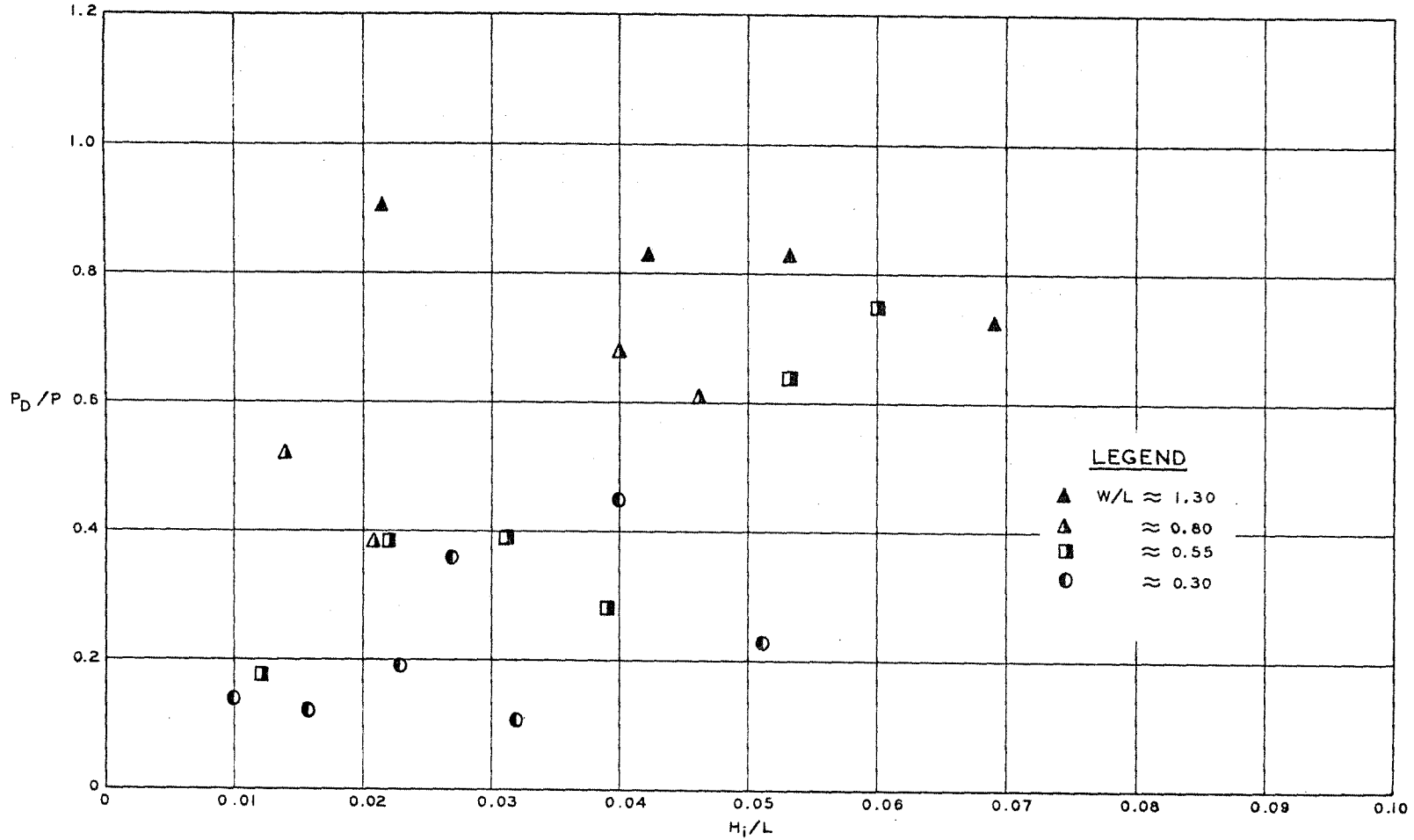

P_D/P VERSUS H_i/L

SPHERE ASSEMBLY

$y/d = 0.6$

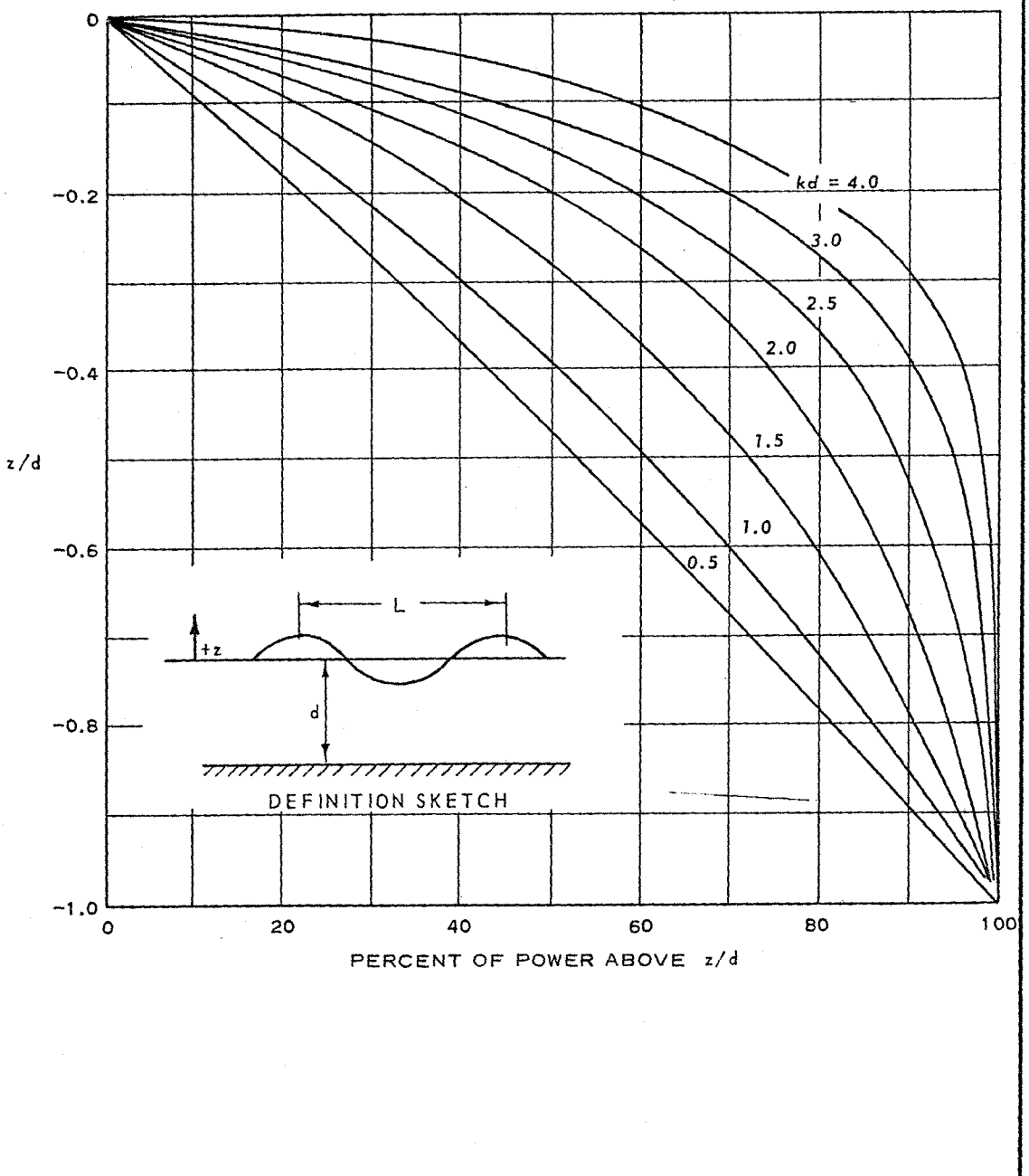

DISTRIBUTION OF
POWER WITH DEPTH

AFTER IPPEN[1]

PLATE 21

PLATE 22

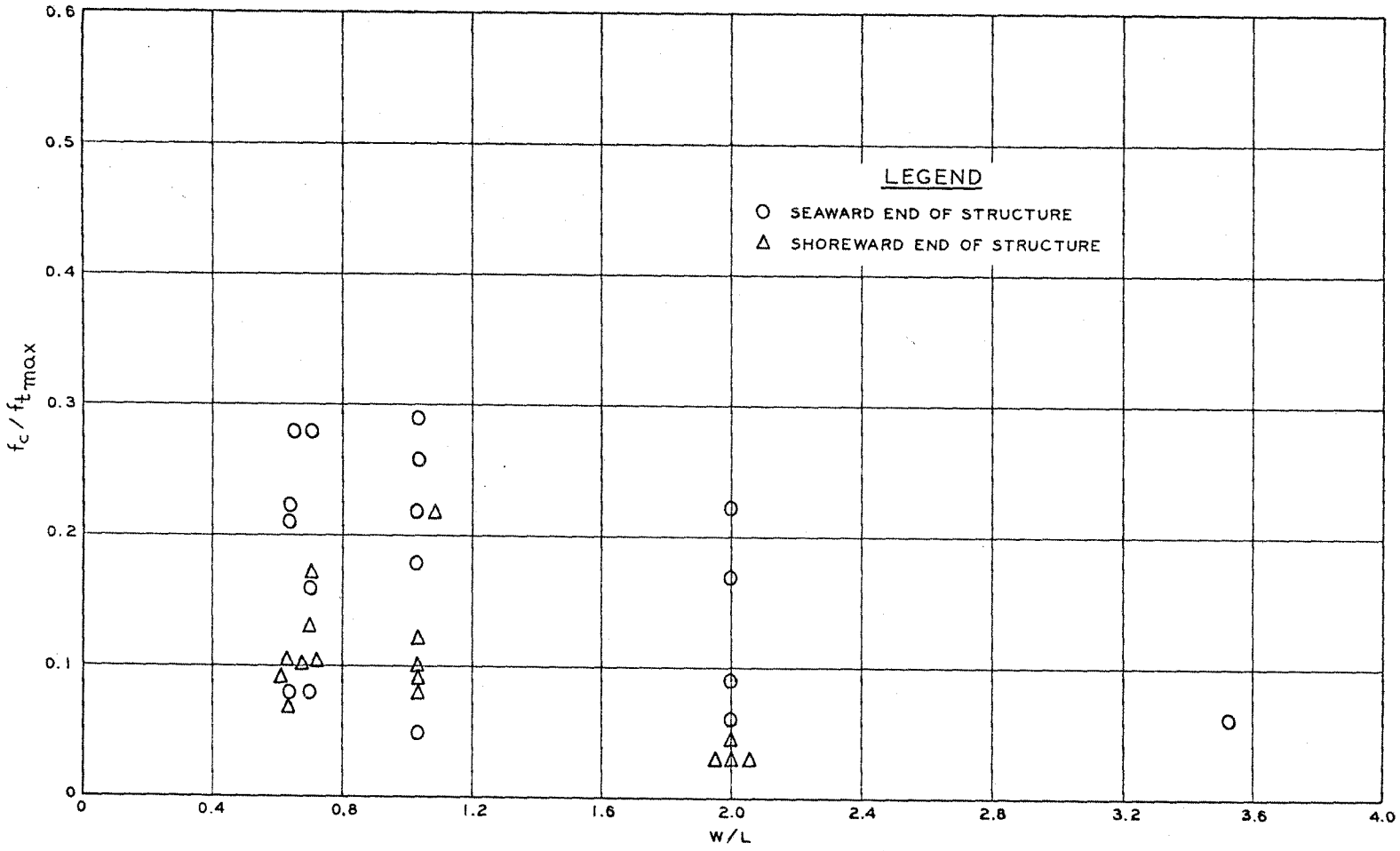

$f_c/f_{t\,max}$ VERSUS W/L

TIRE ASSEMBLY

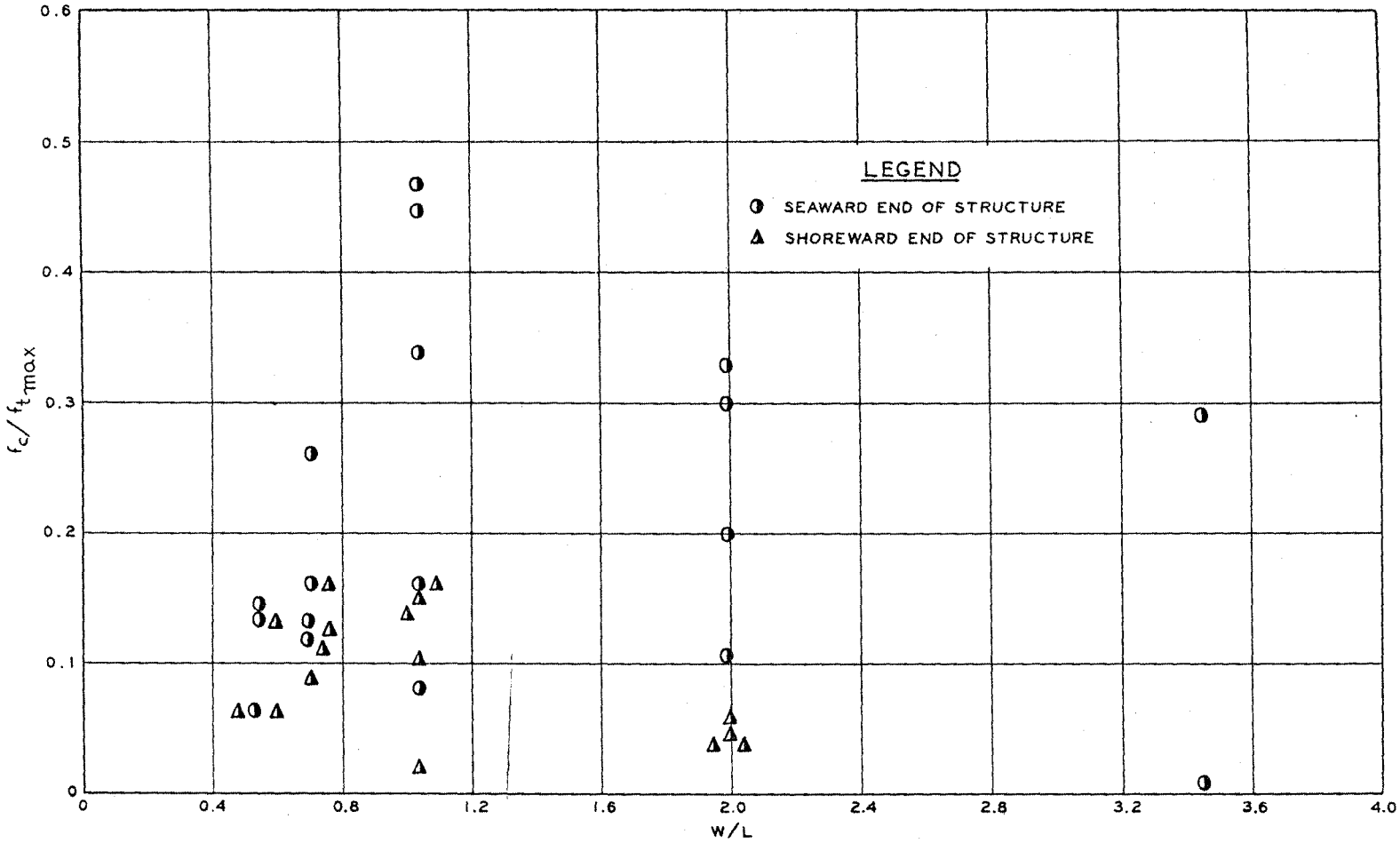

$f_c/f_{t\,max}$ VERSUS W/L

SPHERE ASSEMBLY

Office	No. of Copies	Remarks
OCE (ENGAS-I)	2	
OCE (ENGCW)	2	
OCE (ENGSA)	1	
OCE (ENGTE-E)	1	
Bd of Engrs for Rivers & Harbors	1	
Engr Center, Fort Belvoir	1	
Engr School Library Fort Belvoir	1	
CERC	1	
Supv N. Y. Harbor	1	
LMVD	1	DE
Memphis	1	ATTN: Tech Library
New Orleans	1	ATTN: Hydraulics Br, Engrg Div
St. Louis		Abstract of report to DE Abstract of report to Chief, Hydraulics Br (LMSED-H)
Vicksburg	1	ATTN: Hydraulics Branch
MRD	1	ATTN: Chief, Hydraulics Section
Kansas City	1	ATTN: District Library
Omaha	2	ATTN: Office of Admin Serv (Library)
NAD	1	ATTN: Engineering Division
	1	ATTN: Project Planning Branch
	1	ATTN: Mr. O. F. Reyholec
	1	ATTN: Mr. A. G. Distefano
	1	ATTN: Planning Division
	1	ATTN: Civil Works Br, Constr-Oper Division
	1	ATTN: Mr. Morris Colen

NAD (Continued)		
Baltimore		Abstract of report to DE
	1	ATTN: Engineering Division
	1	ATTN: Planning & Reports Branch
New York	1	ATTN: Engineering Division
	1	ATTN: Basin & Project Planning Branch
Norfolk	1	ATTN: Engineering Division
Philadelphia	1	Engineering Division, ATTN: NAPEN-H
	1	Engineering Division, ATTN: NAPEN-D
NCD	1	ATTN: Library
	1	ATTN: Hydraulics Branch
Buffalo	1	ATTN: Engineering Division
Chicago	1	ATTN: Engineering Division
	1	ATTN: Project & Basin Planning Branch
	1	ATTN: Operations Division
Detroit	1	ATTN: Library
Rock Island	1	DE
St. Paul	1	ATTN: Engineering Division
Lake Survey	3	ATTN: Technical Library
NED	1	ATTN: Hydrology Branch
	1	ATTN: Planning Branch
NPD	1	ATTN: Planning Division
	1	ATTN: Division Hydraulic Laboratory
Alaska	1	ATTN: District Library
	1	ATTN: Hydraulics Design Section
	1	ATTN: Planning & Reports Branch
Portland	1	ATTN: District Library
Seattle	1	ATTN: Engineering Division
	1	ATTN: Planning Branch
Walla Walla	1	ATTN: Engineering Division
	1	ATTN: Planning & Reports Branch

	1	ATTN: Mr. A. J. Moors
Huntington	1	ATTN: Library
	1	ATTN: Hydraulics Branch
Louisville	1	ATTN: Hydraulics Branch
Nashville	1	ATTN: Hydraulics Br, Engrg Division
Pittsburgh	1	ATTN: Engineering Div Tech Library
POD	1	ATTN: Tech Engrg Br, PODGB
Honolulu	1	ATTN: District Library
	1	ATTN: Engineering Division
	1	ATTN: Civil Works Branch
SAD	1	ATTN: Engineering Division
	1	ATTN: Planning Division
Charleston	1	ATTN: Engineering Division
	1	ATTN: Coastal Engineering Branch
Jacksonville	1	ATTN: Project Planning Branch
	1	ATTN: Chief, Canal Hydraulic Section
	1	ATTN: Engineering Division
	1	ATTN: Design Branch
	1	ATTN: Water Management Section
Mobile	1	ATTN: SAMEN-DV
	1	ATTN: SAMEN-P
Savannah	2	ATTN: Planning Branch
Wilmington	1	ATTN: Engineering Division
	1	ATTN: Planning, Reports, & Program Branch
SPD	1	ATTN: Chief, Technical Engineering Branch
	1	ATTN: Planning Division
	1	ATTN: Mr. O. T. Magoon
Los Angeles	1	ATTN: Library
	1	ATTN: Engineering Division
	1	ATTN: Coastal Engineering Branch
	1	ATTN: Mr. R. E. Louden
	1	ATTN: Mr. G. D. Ward
		Abstracts of report to:
		Mr. Edward Koehm
		Mr. Robert S. Perkins
		Mr. Albert P. Gildea
		Project Planning Branch

San Francisco	4	ATTN: Library
D	2	ATTN: Library
Albuquerque	2	DE
Fort Worth	1	ATTN: Librarian
Galveston	1	ATTN: Librarian
	1	ATTN: Engineering Division
	1	ATTN: Project Planning Branch
Little Rock	1	DE
Tulsa	1	DE
S	3	Director
		ATTN: Research Center Library

tomatic:

Engineering Societies Library, New York, N. Y.	1
Library, Div of Public Doc, U. S. Govt Print. Office, Washington, D. C.	1
Library of Congress, Doc Expd Proj, Washington, D. C.	3
COL C. T. Newton	1
Coastal Engrg Research Center, ATTN: Ebba C. Everett, Librarian	1
Prof. J. W. Johnson, Univ of Calif., Berkeley, Calif.	1
Defense Documentation Center, Alexandria, Va.	20

change Basis:

HOUILLE BLANCHE, Grenoble, Grance (ENG-63)	1
The Library, Nat'l Res Council, Ottawa, Canada (ENG-17)	1
The Librarian, Ministry of Technology at Kingsgate House, London, England (ENG-46)	2
The Inst of Civil Engineers, London, England (ENG-47)	1
Inst of Engineers, Sidney, Australia (ENG-162)	1
APPLIED MECHANICS REVIEWS, San Antonio, Tex.	2
Dept of Civil Engineering, The Univ of Arizona, Tuscon, Ariz.	1
Dr. Donald A. Sawyer, Auburn Univ, Auburn, Ala.	1
Bureau of Reclamation	1
Prof. A. J. Acosta, Hydrodynamics Lab, Calif. Inst of Tech, Pasadena, Calif.	1

Exchange Basis: (Continued)

Scripps Inst of Oceanography, Univ of Calif., LaJolla, Calif.	1
Engrg Lib, Univ of Calif., Berkeley, Calif.	1
Central Records Library, Dept of Water Resources, Sacramento, Calif.	1
W. M. Keck Lab of Hydraulics & Water Resources, Calif. Inst of Tech, Pasadena, Calif.	1
Case Inst of Tech, Cleveland, Ohio	1
Central Serial Record Dept, Cornell Univ Lib, Ithaca, N. Y.	1
Engrg & Ind Experi Sta, Univ of Florida, Gainesville, Fla.	1
Price Gilbert Memorial Library, Georgia Inst of Tech, Atlanta, Ga.	1
Gordon McKay Library, Cambridge, Mass.	1
Gift & Exchange Division, Univ of Ill. Library, Urbana, Ill.	1
Library, Iowa State Univ of Science & Tech, Ames, Iowa	1
Engrg Experi Sta, Kansas State Univ of Agric & Applied Science, Manhattan, Kans.	1
Documents Room, Univ Lib, Univ of Kansas, Lawrence, Kans.	1
Fritz Engineering Lab, Lehigh Univ, Bethlehem, Pa.	1
Hydrodynamics Laboratory, MIT, Cambridge, Mass.	1
University of Arkansas, Fayetteville, Ark.	1
Mr. Robert T. Freese, Univ of Michigan, Ann Arbor, Mich.	1
Engineering & Ind Research Sta, State College, Miss.	1
College of Engineering, Univ of Missouri, Columbia, Mo.	1
Univ of Missouri, School of Mines & Metallurgy, Rolla, Mo.	1
North Carolina State College, Raleigh, N. C.	1
Dept of Civil Engrg, Technological Inst, Northwestern Univ, Evanston, Ill.	1
Main Library, Ohio State Univ, Columbus, Ohio	1
Engrg Experi Sta, Oregon State Univ, Corvallis, Oreg.	1
Dept of Oceanography, Oregon State Univ, Corvallis, Oreg.	1
New York University, ATTN: Engrg Lib, University Heights, Bronx, N. Y.	1
McGill University, Montreal, Quebec, Canada (ENG-271)	1
Engrg Library, Pennsylvania State Univ, University Park, Pa.	1
Periodicals Checking Files, Purdue Univ Libraries, Lafayette, Ind.	1
Tennessee Valley Authority	1
Research Editor, Texas Transportation Inst, Texas A&M Univ, College Station, Tex.	1
Office of Engineering Research, Publications, Univ of Washington, Seattle, Wash.	1
Albrook Hydraulic Lab, Washington State Univ, Pullman, Wash.	1
Engrg Lib, Univ of Wisconsin, Madison, Wis.	1
Engineering Library, Stanford University, Stanford, Calif.	1
Serials Acquisitions, Univ of Iowa Libraries, Iowa City, Iowa	1
Lorenz G. Straub Memorial Library, Minneapolis, Minn.	1
Director, Pacific Region, Dept of Public Works, Vancouver, B. C., Canada (ENG-318)	1

Abstract of Report:
CG, Fourth U. S. Army, Fort Sam Houston, Tex., ATTN: AKAEN-OI
Princeton University River & Harbor Library, Princeton, N. J.
Duke University Library, Durham, N. C.
Princeton University Library, Princeton, N. J.
Louisiana State University Library, Baton Rouge, La.
The Johns Hopkins University Library, Baltimore, Md.
University of Kansas Libraries, Lawrence, Kans.
Laboratorio Nacional de Engenharia Civil, Lisboa, Portugal
Dept of Civil Engrg, Univ of Tokyo, Bunkyo-ku, Japan
Mr. Shigematsu Suzuki, Civil Engrg Res Inst, Hokkaido Development Bureau, Nakanoshima, Sappo, Japan
Commandant, USAREUR Engineer-Ordnance School, APO New York 09172
Mr. J. C. Harrold, 4216 Pennsylvania Ave., Apt. 2, Kettering, Ohio
Water Information Center, Inc., Water Research Bldg, 44 Sintsink Drive, East, Port Washington, N. Y.
Duke University, College of Engineering Library, Durham, N. C.
Serials Record, Pennsylvania State University, University Park, Pa.

Send with Bill:
Librarian, Dept of Public Works, Sydney, Australia 1

Announcement of Availability by Tech Liaison Branch:
CIVIL ENGINEERING
THE MILITARY ENGINEER
ENGINEERING NEWS-RECORD

Unclassified
Security Classification

DOCUMENT CONTROL DATA - R & D

(Security classification of title, body of abstract and indexing annotation must be entered when the overall report is classified)

1. ORIGINATING ACTIVITY *(Corporate author)*
U. S. Army Engineer Waterways Experiment Station
Vicksburg, Mississippi

2a. REPORT SECURITY CLASSIFICATION
Unclassified

2b. GROUP

3. REPORT TITLE
HYDRAULIC CHARACTERISTICS OF MOBILE BREAKWATERS COMPOSED OF TIRES OR SPHERES; Hydraulic Laboratory Investigation

4. DESCRIPTIVE NOTES *(Type of report and inclusive dates)*
Final report

5. AUTHOR(S) *(First name, middle initial, last name)*
Adel M. Kamel
D. Donald Davidson

6. REPORT DATE	7a. TOTAL NO. OF PAGES	7b. NO. OF REFS
June 1968	70	13

8a. CONTRACT OR GRANT NO.	9a. ORIGINATOR'S REPORT NUMBER(S)
b. PROJECT NO.	Technical Report H-68-2
c.	9b. OTHER REPORT NO(S) *(Any other numbers that may be assigned this report)*
d.	

10. DISTRIBUTION STATEMENT
Each transmittal of this document outside the agencies of the U. S. Government must have prior approval of Office, Chief of Engineers.

11. SUPPLEMENTARY NOTES	12. SPONSORING MILITARY ACTIVITY
	Office, Chief of Engineers U. S. Army Washington, D. C.

13. ABSTRACT

Two new types of mobile breakwaters consisting of tire and sphere assemblies, respectively, were tested. Tests covered a wide range of wave conditions, water depths, and breakwater dimensions. Experimental measurements were made to determine the wave reflection and wave transmission coefficients, the power dissipated by the breakwaters, and the forces in the mooring lines of the breakwaters. It was found that for these types of floating breakwaters to be effective their length should be on the order of one-half to one wavelength, their depth on the order of half the water depth, and the wave steepness equal to or greater than about 0.04. The effectiveness of these breakwaters can be improved by decreasing their porosity and flexibility; however, this would cause an increase in the mooring forces and the drift, the drift being the result of the difference between the forces in the seaward and shoreward mooring lines.

DD FORM 1 NOV 68 1473 REPLACES DD FORM 1473, 1 JAN 64, WHICH IS OBSOLETE FOR ARMY USE.

Unclassified
Security Classification

14. KEY WORDS	LINK A		LINK B		LINK C	
	ROLE	WT	ROLE	WT	ROLE	WT
Breakwaters						
Floating breakwaters						
Spheres						
Tires						